Title:

Metal toxicity contributes to the structuring of bacterial communities in the Arabidopsis leaf phyllosphere

Author names and affiliations:

Jan F. Plewka-Mandelkow[1], Anna S. Thomas[1], Julia A. Vorholt[2], Ute Krämer[1§]

[1]Faculty of Biology and Biotechnology, Ruhr University Bochum, 44801 Bochum, Germany
[2]Institute of Microbiology, ETH Zurich, Zurich, Switzerland

[§]**Corresponding author**: Ute.Kraemer@ruhr-uni-bochum.de
Professor Dr. Ute Krämer
Molecular Genetics and Physiology of Plants
Ruhr University Bochum
Universitätsstraße 150, Box 44, ND3/30
D-44801 Bochum, Germany
Tel.: +49 (0)234 32 24291, FAX: +49 (0)234 32 14187

One sentence summary: Based on the magnitude and variation of metal tolerances among bacterial strains of the Arabidopsis phyllosphere, we conclude that common leaf apoplastic cadmium and zinc concentrations can influence bacterial community structure.

List of author contributions: U.K. conceived the project, J.F.P.-M. and U.K. designed research with contributions from J.A.V., J.F.P.-M. and A.T. performed experiments, J.A.V. contributed materials, J.F.P.-M., A.T., and U.K. analyzed data, J.F.P.-M. and U.K. wrote the manuscript, with contributions from J.A.V. All authors read and edited the manuscript.

Funding information: This work was supported by Ruhr University Bochum, Germany, and the Deutsche Forschungsgemeinschaft (RTG 2341 Microbial Substrate Conversion).

Highlights

- Metal(loid) sensitivities of the *Arabidopsis thaliana* phyllosphere bacterial strain (*At*-LSPHERE) collection followed the order of toxicity Cd^{2+} >> Cu^{2+} > Zn^{2+} > arsenite (As^{III}) > Mn^{2+} > arsenite (As^{V}), whereby the responses of individual strains were uncorrelated between metal(loids) and predicted the sensitivities of multi-strain synthetic communities.

- Upon cultivation of Arabidopsis in unpolluted soil, total Cd^{II} and Zn^{II} in leaf apoplastic fluid were equivalent to concentrations that arrested growth of up to 2.2% and 0.4% of phyllosphere bacterial strains on agar-solidified R2A medium, respectively, whereas apoplastic Cu^{II} and Mn^{II} were 10- to 100-fold below bacteriotoxic levels.

- Phyllosphere bacteria known to strongly influence community composition mostly remained highly sensitive under combined metal(loid) exposure, and elevated tolerances to Cd^{II} and Zn^{II}, but not to other metalloid(s), in phyllosphere compared to soil bacteria were consistent with divergent natural selection in the leaf and soil environments.

- The degree of phyllosphere bacterial metal(loid) tolerances correlates with the presence and copy number of known tolerance genes, with genus accounting for 63% of the variation in gene content and 42% of the phenotypic variation in metal(loid) tolerance.

- In summary, our data suggest that local Cd and Zn levels in the Arabidopsis leaf endosphere influence the composition of bacterial communities and have shaped their phenotypic metal(loid) tolerance properties as a result of natural selection.

Abstract

Diversity and composition of plant-associated microbiota are attributed to host and microbial genotype as well as the environment, yet our understanding of the causal factors driving these patterns remains incomplete. Elevated concentrations of the micronutrients zinc (Zn), manganese (Mn) and copper (Cu), and exposure to non-essential trace elements including cadmium (Cd) and arsenic (As), can be toxic. Here we explored whether differences in metal(loid) homeostasis between plants and bacteria shape microbial community composition in the phyllosphere. Among the biologically relevant metal(loid)s Cd, Cu, Mn, Zn, and As, we identified Cd^{II} as the most toxic, and As^{V} (arsenate) as the most harmless, by screening 224 representative *Arabidopsis thaliana* phyllosphere bacterial strains on metal(loid) concentration series in synthetic media. Comparing bacteriotoxicity profiles with our measurements of the leaf apoplastic fluid ionome indicated that Zn^{2+} and Cd^{2+} concentrations are the most likely to arrest growth of metal-sensitive strains *in planta*. Soil bacterial strains were several-fold more sensitive to both these metals than leaf strains, consistent with selection for increased bacterial Zn and Cd tolerance in the phyllosphere. Keystone strains, known to govern bacterial community structure, were highly metal-sensitive, with only few between-metal interactions and no between-strain interactions modulating single-metal(loid) toxicities. Overall, bacterial genus explained 63% of the variance in metal(loid)-related gene content and 42% of the metal(loid) tolerance phenotypic variance. Cd tolerance correlated with the presence and copy number of known Cd-related genes. In summary, our results support the hypothesis that plant metal homeostasis contributes to structuring bacterial communities in the leaf endosphere.

Keywords

Arabidopsis thaliana, leaf apoplast, phyllosphere, synthetic communities, cadmium, zinc, microbiome

1. Introduction

Diversity among bacteria is unparalleled, and they have colonized the broadest range of habitats in the world, including soil, water, and multicellular organisms. The plant-associated microbiota comprises complex microbial communities influenced by the plant host, microbe-microbe interactions, and other environmental factors, and can have positive effects on plant fitness (Müller, Vogel, et al. 2016; Ritpitakphong et al. 2016; Vogel et al. 2021). Leaves provide two distinct microbial habitats: one on the leaf surface named the phylloplane, and one inside the leaf comprising the apoplast, named the endosphere. One of the largest habitats for bacteria is the leaf surface, with an estimated global area of around 1 billion km^2 (Vorholt 2012). From the surface of a leaf, the leaf endosphere is accessible *via* the stomata while they are open. Within a given plant organ, the volume outside the plasma membranes bordering all cells is referred to as the apoplast, comprising both the cell walls and the intercellular space in between (Sattelmacher 2001). In general, the leaf apoplast is at least partially filled with an extracellular solution, and the remainder of it is occupied by air. In addition to its role as a habitat for microbial communities, the apoplast serves as a site for the inter-cellular movement of gases, water and solutes, as well as for the storage and detoxification of organic and inorganic compounds including metals (Küpper et al. 2000; Sattelmacher 2001; Kajala et al. 2019).

Impacts on bacteria inhabiting the phylloplane, rhizosphere and rhizoplane are determined predominantly by the environment around the plant. The closer the plant host, the stronger is its influence on the microbiota (Chen et al. 2020; Bulgarelli et al. 2013). The plant begins to exert some control over the composition of its apoplast progressively from the root epidermis inwards, where both diffusion from the soil solution and microbial colonization can occur easily on the external side of, or during root developmental stages prior to the formation of, apoplastic barriers. In roots, apoplastic barriers are constituted by the Casparian strip that is positioned radially around root endodermal cells as well as the suberization of the outwardly oriented surfaces of epidermal and endodermal cell layers, both initiated at specific stages of cellular differentiation. Endodermal suberization is plastic to some degree and regulated dependent on both the plant's nutritional status and plant-associated microbial communities (Barberon et al. 2016; Robb et al. 1991; Andersen, Barberon, and Geldner 2015). The apoplast on the internal side of the root apoplastic barriers and of the leaf endosphere represent comparably sheltered niches for the inhabiting microbes. At these sites, the plant host has a

107 predominant influence on apoplast composition, thus providing opportunities for niche
108 construction by the plant. To date, little is known about the composition of this micro-habitat
109 and any evolutionary adaptations to it in the inhabiting microbes.

110 The plant apoplast is known to function in the storage and detoxification of excess metal
111 cations, including those of so-called heavy metals, or – more accurately – class B (e.g., Cu^{+})
112 and borderline elements (e.g., Cu^{2+}, Cd^{2+}, Fe^{2+}, Fe^{3+}, Mn^{2+}, Zn^{2+} (Nieboer 1980; Farvardin et
113 al. 2020)). Among these, the micronutrients (mostly Fe, Zn, Cu, Mn and Ni) are required in
114 small quantities by all organisms to serve as or within protein cofactors acting in ligand binding
115 and in the catalysis of a variety of chemical reactions (Pais and Jones 1997; Marschner and
116 Marschner 2012). Because of their powerful chemical properties, these same nutrients can
117 become highly toxic even when present in slight excess. Moreover, chemically similar non-
118 essential metallic trace elements are ubiquitously present in the environment, for example Cd.
119 All organisms, including bacteria and plants, possess metal homeostasis networks which
120 operate to fulfill nutritional metal requirements while counteracting metal toxicities across their
121 specific environmental ranges (Clemens 2001; Nies and Grass 2009; Chandrangsu, Rensing,
122 and Helmann 2017). Over the course of evolution, metal homeostasis networks, as well as
123 nutritional metal needs, have diverged between bacteria, fungi and plants to some extent. For
124 example, the metalloproteome of plants generally requires more Cu and Zn, and less Ni, than
125 that of most bacteria (Williams 2007). This divergence implies that metal concentrations
126 maintained and tolerated by the plant within the apoplast may be inhibitory to bacterial
127 colonists, raising the possibility that plants modulate apoplastic metal levels to selectively
128 influence microbial community composition. In support of this, *Arabidopsis thaliana* Zn^{2+}
129 efflux ATPases HMA2 and HMA4 are required for resistance to the necrotrophic fungal
130 pathogen *Plectosphaerella cucumerina*, demonstrating that plant-controlled apoplastic metal
131 levels can shape interactions with microbial colonists (Escudero et al. 2022). This concept
132 parallels nutritional immunity—a process well-established through medical research where the
133 host manipulates nutrient availability to limit pathogen growth—yet it remains underexplored
134 in plant science (Murdoch and Skaar 2022; Krämer 2024).

135 Here we explore the relationship between metal(loid) levels in the plant apoplast and plant-
136 associated microbial communities. We profiled the metal(loid) tolerances of 224 representative
137 phyllosphere bacterial strains of the *At*-LSPHERE collection, a curated set of isolates from the
138 model plant *A. thaliana* (Bai et al. 2015), focusing on elements that could reach bacteriotoxic

139 levels inside leaves of plants in their natural non-contaminated environments: Cd, Cu, Mn, Zn,
140 and arsenic. We then generated ionomic data for the Arabidopsis leaf apoplast for an evaluation
141 in the context of phyllosphere bacterial metal(loid) tolerances as well as in comparison to
142 tolerance profiles of soil bacteria, and we identified genomic predictors of metal tolerance in
143 phyllosphere bacterial strains. Taking our findings together, we assessed whether metal(loid)
144 co-tolerance patterns reflect shared chemical properties or environmental selection. In
145 summary, our work identifies the modulation of Zn and Cd levels in the leaf apoplast as a
146 potential means for plants to shape the bacterial community in their leaf endosphere.

147 # 2. Results

148 **2.1 Profiles of metal(loid) tolerances among Arabidopsis phyllosphere bacterial strains**

149 It is presently unknown whether the metal levels in the leaf apoplast can influence the
150 composition of phyllosphere microbial communities. To obtain information for addressing this
151 question, we profiled the metal(loid) tolerance limits of all individual strains within the publicly
152 available representative collection of Arabidopsis leaf phyllosphere bacteria named *At*-
153 LSPHERE (n = 224) (Bai et al. 2015). For comparison, we additionally profiled a publicly
154 available collection of bacteria from unplanted soil (n = 33) (Bai et al. 2015). We spotted
155 bacterial suspensions of each strain on agar-solidified R2A media supplemented with
156 concentration series of the essential metals copper^{II} (Cu^{II}), zinc^{II} (Zn^{II}), and manganese^{II} (Mn^{II}),
157 as well as of the non-essential trace metal cadmium^{II} (Cd^{II}), and the metalloid arsenic (As) in
158 two common inorganic forms, arsenite (As^{III}) and arsenate (As^{V}) (Tables S1 to S3).

159 Cd^{II} was toxic for some *At*-LSPHERE strains at the lowest tested concentration (1.5 µM).
160 Concentrations of 4.3 µM Cd and 49 µM Cd eliminated the growth of 5% and 50% of the
161 bacterial strains, respectively (termed here Effective Concentrations EC_5 and EC_{50}), with a
162 factor of 130 between the Cd concentrations eliminating the 5% most sensitive (EC_5) and the
163 5% most tolerant strains (EC_{95}; based on curve fits, defined here as concentration range; Figure
164 1A, Table 1). Compared to phyllosphere bacterial strains, soil bacteria were more sensitive to
165 Cd, with EC_5, EC_{50} and EC_{95} concentrations of approximately 50%, 20% and 10%,
166 respectively, and only about one-fifth of the concentration range (Figure 1B, Table 1).

167 We observed EC_{50} values of 0.42, 0.57, and 1.1 mM, respectively, for the trace elements Cu^{II},
168 Zn^{II}, and arsenite (As^{III}). Of these three elements, Zn began to impede the growth of some

169 phyllosphere bacterial strains at the lowest tested concentration of 50 µM (EC_5 of 83 µM), and
170 it continued to permit the growth of the most tolerant strains up to the highest concentration
171 (EC_{95} of 11 mM; Figure 1A, Table 1), with a concentration range of 130, very similar to that
172 for Cd. Soil bacteria were less Zn-tolerant, showing EC_5, EC_{50} and EC_{95} concentrations of
173 approximately 40%, 30% and 6%, respectively, and only about one-eighth of the concentration
174 range, compared to phyllosphere bacteria (Figure 1B, Table 1).

Table 1. Effective concentrations of metals on collections of bacterial strains (based on curve fits).

***At*-LSPHERE bacterial strain collection**				
Element	**EC_5 [mM][a]**	**EC_{50} [mM][a]**	**EC_{95} [mM][a]**	**Concentration range[c]**
Cd^{II}	4.3×10^{-3}	0.049	0.56	130
Cu^{II}	0.11	0.42	1.6	15
Zn^{II}	0.083	0.57	11	130
As^{III}	0.17	1.1	6.6	39
Mn^{II}	3.0	9.2	85	28
As^{V}	~0.1[b]	> 100[b]	> 100[b]	>> 100[b]
Soil bacterial strain collection				
Element	**EC_5 [mM][a]**	**EC_{50} [mM][a]**	**EC_{95} [mM][a]**	**Concentration range[c]**
Cd^{II}	2.0×10^{-3}	0.010	0.054	27
Cu^{II}	0.25	0.60	1.4	5.6
Zn^{II}	0.040	0.16	0.66	17
As^{III}	0.087	1.1	14	160
Mn^{II}	0.77	15	> 100[b]	>> 100[b]
As^{V}	~0.1[b]	> 20[b]	> 100[b]	>> 100[b]

[a]EC_n denote metal concentration preventing growth of *n*% of the tested bacterial strains. Values based on curve fits, see Figure 1A, Data S1 and Methods).
[b]Values estimated from experiments (no curve fit possible).
[c]Ratio EC_{95}: EC_5

175 The 15-fold difference in Cu concentration between the EC_5 of 0.11 and the EC_{95} of 1.6 mM
176 was the narrowest among all metal(loid)s tested in phyllosphere bacteria. Compared to
177 phyllosphere bacteria, soil bacteria were more Cu-tolerant, with approximately 2-fold EC_5, 1.5-
178 fold EC_{50}, and a similar EC_{95} (around 90%), despite a narrower concentration range of
179 approximately one-third of that observed in phyllosphere bacteria. Consequently, the largest
180 differences between phyllosphere and soil bacteria were observed among EC_{95} values: *ca*. 20-
181 fold higher for Zn and 10-fold for higher for Cd.

182 Arsenite was less toxic to phyllosphere bacteria than Cd^{II}, Cu^{II}, and Zn^{II}, with an EC_{50} of 1.1
183 mM (Figure 1A, Table 1). The EC_{50} of Mn^{II} was as high as 9.2 mM, and arsenate was the least

184 harmful to *At*-LSPHERE strains. At the highest tested arsenate concentration of 100 mM, about
185 50% of the bacterial strains were still able to grow, although we depleted phosphate in these
186 media (Tables S1 to S3). For these metal(loid)s, phyllosphere bacteria tended to have higher
187 EC_5 concentrations than soil bacteria (about 2-fold for As^{III} and 4-fold for Mn^{II}), similar EC_{50}
188 concentrations, and phyllosphere bacteria had lower EC_{95} concentrations than soil bacteria,
189 clearly different from Zn, Cd and Cu (Figure 1A and B, Table 1). These results suggested that
190 bacterial strains with elevated Cd^{II} and Zn^{II} tolerance are enriched in the phyllosphere of
191 Arabidopsis compared to unplanted soil under natural field conditions.

192 We next investigated whether the metal tolerances of single strains are representative of those
193 of bacterial communities, using Cd tolerance as an example. We designed three synthetic
194 communities (SynComs) comprising strains that individually exhibited high, intermediate and
195 low Cd tolerance, respectively (Table S4). The composition of these SynComs matched the
196 phylogenetic profile of phyllosphere communities as closely as possible (Figure S1). On solid
197 R2A media, growth of the SynComs reflected that of the most tolerant strain in single-strain
198 assays (Figure S2A and S2B). The relative Cd tolerances of SynComs in liquid R2A media
199 also qualitatively followed the relative Cd tolerances of single strains observed on solid media.
200 Cd toxicity was more severe in liquid media, with growth decreases observed at the lowest
201 tested Cd concentration of 1.5 µM in both the sensitive and the intermediate SynCom, and a
202 complete growth arrest of the sensitive SynCom as well as strongly attenuated growth of the
203 intermediate and tolerant SynComs at 15 µM Cd (Figures 1C and S3, compare with Fig. S2
204 and Table 1; growth arrest only of the sensitive SynCom at 240 µM on solid R2A media).
205 Taken together, these results supported the relevance of our single-strain tolerance assays in
206 exemplary bacterial communities.

207 **2.2 Magnitudes of apoplastic Cd and Zn concentrations reach levels toxic to a subset of**
208 **phyllosphere bacterial strains**

209 To address whether any members of phyllosphere bacterial communities might ever encounter
210 toxic metal levels in the leaf endosphere, we examined the composition of the leaf apoplastic
211 fluid (AF). Apoplastic wash fluid (AWF) was extracted from the leaves of seven- to eight-
212 week-old soil-grown *A. thaliana* plants (Tables S5 and S6) using the infiltration-centrifugation
213 method (O'Leary et al. 2014; Figueiredo et al. 2021). Plant cultivation was conducted on a
214 standard greenhouse soil, with an additional experiment using a field-collected soil from a
215 region known for geogenically slightly elevated total Cd levels for comparison (Stein et al.

216 2017). AWF is commonly obtained using water as an infiltration fluid (IF). IF might affect
217 metal solubility during the experimental procedure, for instance by increasing the local
218 extracellular pH within infiltrated leaves. Therefore, we interpret the corresponding results as
219 estimates of the minimal metal levels encountered in the AF. Our current understanding of
220 metal partitioning within plants implies that cell walls contain bound metal cations, which
221 continuously equilibrate with the surrounding AF and can thus affect the microbes in this
222 compartment. To obtain AWF containing what we interpret as estimates of the maximal metal
223 concentrations in the leaf AF of plants cultivated under the conditions employed, we used as
224 the IF a solution of 100 µM ethylenediaminetetraacetic acid (EDTA). EDTA is a synthetic
225 chelator of metal cations, with affinities following the sequence of $Fe^{3+} > Cu^{2+} >> Zn^{2+} > Fe^{2+}$
226 $> Mn^{2+} >> Mg^{2+} > Ca^{2+}$ (Norvell 1991), and it can thus be predicted to mobilize the readily
227 available fraction of transition metal cations from cell walls and other binding sites.

228 Carrying out the infiltration-centrifugation protocol with insufficient caution can damage cell
229 integrity, thus causing cytoplasmic contamination of the AWF. Therefore, we generated
230 additional control samples in which we intentionally provoked cytoplasmic contamination by
231 inflicting mechanical stress on the leaves through harsh handling during the experimental
232 procedure at three levels of severity (little, intermediate, and strong damage). We quantified
233 the concentrations of multiple elements in all AWF samples by ICP-OES and subsequently
234 calculated the concentrations of nutrient elements and Cd in AF *in vivo* (see Methods). A
235 principal component analysis (PCA) of the ionomic profiles of all AWF samples demonstrated
236 that provoked cytoplasmic contamination is associated with strongly elevated concentrations
237 of calcium (Ca), potassium (K), magnesium (Mg), sulfur (S), and phosphorus (P) (Figure S4A,
238 PC 1 separates the experimental samples from the control samples obtained after intentionally
239 inflicting cell damage). Consequently, a PCA of ionomic profiles is a sensitive means to detect
240 cytoplasmically contaminated AWF samples, all of which were excluded from further analysis
241 (Figure S4A and B). Notably, neither Cd nor Zn concentrations were increased upon provoking
242 cytoplasmic contamination (Figure S4A), supporting their predominantly apoplastic – and not
243 cytoplasmic – origin in our AWF samples.

244 Compared to total concentrations across entire hydrated leaves, nutrients (Fe, Mo, Cu, Ca, S,
245 P, Mg, and K) were generally depleted in AF, most strongly for Fe. By comparison to bulk
246 leaves, there was an enrichment in AF of Mn, Cd and Zn (Figure 1D, see also Figure S4C and
247 D), consistent with the preferential sequestration of these elements in the apoplastic

248 compartment. Overall, only a minor proportion of the total amount of all elements was
249 extracted from leaves in the AWF (Table S7). We calculated Cd and Zn concentrations in
250 AF_{EDTA} to be at least 0.07 and 5.2 µM, and up to 0.4 and 40 µM, respectively, with considerable
251 variability between replicate samples and independent experiments (Table S5, Figure 1E,
252 Figure S4E-G). Accordingly, the range of Zn concentrations in the AF included concentrations
253 capable of preventing the growth of the most sensitive bacterial strains when tested on solid
254 R2A medium. Cd concentrations in AF closely approached these magnitudes (Table 1; Figure
255 1E), although plants were grown on greenhouse soil containing only trace levels of Cd (total
256 Cd < 0.1 mg kg^{-1}; Table S6). Cd and Zn concentrations in AF were elevated in the presence of
257 EDTA in the IF, suggesting that EDTA mobilized pools of both metals from extracellular
258 binding sites within infiltrated leaves (Figure 1E, Table S5, Figure S4A, PC 2 separates
259 samples obtained with EDTA from those obtained with water as the extraction fluid). It should
260 be noted that we consider the direct quantitative comparison between metal concentrations in
261 AF and R2A medium merely as a first reasonable approximation (see also Discussion).

262 In contrast to Cd and Zn, total concentrations of Cu and Mn in the AF of approximately 1 and
263 70 µM, respectively, were far below toxic levels in the R2A medium of ≥ 0.1 and ≥ 3 mM for
264 Cu and Mn, respectively (Figure 1A, Table 1). Overall, Cu concentrations in AF were
265 independent of whether we used EDTA solution or water as IF, suggesting that negligible
266 proportions of the apoplastic Cu pool were reversibly bound to cell walls of infiltrated leaves
267 (Figure 1D, Figure S4G, Table S5). In summary, these results indicated that Cd and Zn are
268 enriched in the leaf apoplast and have the potential to directly attenuate or eliminate the growth
269 of a subset of leaf phyllosphere bacteria.

270 **2.3 Towards extrapolating how metals affect phyllosphere bacterial community**
271 **composition**

272 Previously published drop-out experiments with synthetic bacterial communities of *A. thaliana*
273 showed that the absence of single bacterial strains, such as L203-*Microbacterium*, L231-
274 *Sphingomonas*, L233-*Rhodococcus,* and L262-*Rhizobium*, can alter the structures of bacterial
275 communities (Carlström et al. 2019). These strains are thus referred to as keystone strains
276 (Carlström et al. 2019). In these keystone strains, maximum permissive concentrations (MPC)
277 were often larger or equal to *At*-LSPHERE-wide EC_{50}, with strain-specific sensitivities to
278 individual metal(loid)s (MPC < EC_{50}; Cu^{II}: L262, Mn^{II}: L231, Zn^{II}: L262 and L231, arsenite:
279 L203 and L262, Cd^{II}: all except L262; Data S1) so that none of these strains shared an identical

280 profile with any other strain. This suggested that metal tolerances in keystone strains reflect
281 distinct evolutionary histories rather than a shared chemical response. L233 was the most Cd-
282 sensitive, with a maximum permissive concentration (MPC) of 1.5 μM Cd (the lowest
283 concentration tested on solid R2A media; 3% of the EC_{50} of 49 μM Cd, see Figure 2A and
284 Table 1). Keystone strains L203 and L231 were also Cd-sensitive (MPC at 30% of EC_{50}).
285 Compared to these Cd concentrations, the maximal Cd concentration in AF (0.4 μM) was lower
286 (see Figure 1E, Table S5). In subsequent experiments we observed that even a concentration
287 of 0.5 μM Cd in liquid R2A medium fully suppressed the growth of L203 and caused a mild
288 growth reduction on L231 and L233 (Table S8). Keystone strain L262 was sensitive to Cu^{II},
289 arsenite and Zn^{II} (MPCs at ≤ 40% of EC_{50}), and tolerant to Cd^{II} (MPC 490% of EC_{50}) (Figure
290 2A). Besides its sensitivity to Cd^{II} (see above) and As^{III} (MPC 23% of EC_{50}), keystone strain
291 L203 showed moderately elevated tolerance to Cu (MPC 140% of EC_{50}) and Zn (MPC 180%
292 of EC_{50}). Cd-sensitive keystone strains L231 and L233 (see above) had some degree of Cu
293 (140% of EC_{50}) and As^{III} (230% of EC_{50}) tolerance, with additional Zn tolerance in L233
294 (350% of EC_{50}).

295 Next, we tested for possible combined effects of metals on the keystone strains. We examined
296 the effects of combining Cd^{II} and Cu^{II}, and of combining Cd^{II}, Zn^{II}, and Mn^{II} in the liquid
297 culture system (Figure 2B and C). The highest tested concentration of Cu^{II} was substantially
298 more toxic to L233 and L262 in the presence of Cd^{II}, implying synergistic toxicity of Cd^{II} and
299 Cu^{II} (Figure 2B, Table S8). A mild growth reduction appeared at concentrations of 0.5 μM Cd^{II}
300 or 100 μM Cu^{II}, whereas the combination of 0.5 μM Cd^{II} and 100 μM Cu^{II} completely
301 eliminated the growth of L233. Similarly, neither Cd^{II} nor Cu^{II} alone were heavily toxic to
302 L262 at the tested concentrations, whereas the combination of 100 μM Cu^{II} with any of the
303 tested Cd^{II} concentrations exacerbated the toxic effects. In contrast, combined treatments
304 appeared to alleviate toxicity in L231 when compared to treatments with Cd^{II} and Cu^{II} alone
305 (Figure 2B, Table S8). Reproducible combined effects were largely restricted to Cu^{II}
306 concentrations in liquid R2A media that were 14- to 300-fold higher than in AF (see Table S5).

307 In experiments combining up to three metals, the single Zn^{II} concentration tested (50 μM) alone
308 tended to decrease the growth of L203 and L231, and more strongly of L233 and L262 (Table
309 S9). The tested Mn^{II} concentration (10 μM) alone had no consistent effects on the growth of
310 keystone strains (Table S9). When tested in combination with varying concentrations of Cd^{II}
311 (0.5, 5 and 20 μM), Zn^{II} exacerbated the toxicity of all Cd^{II} conditions in strain L262, which

312 was highly tolerant to Cd alone, whereas Mn^{II} alleviated both the single and combined
313 toxicities of Zn^{II} and Cd^{II} to this strain (Figure 2C). Zn^{II} also tended to exacerbate the toxicity
314 of Cd^{II} in L231, and it exacerbated the toxicity of Mn^{II} in L203. Mn^{II} tended to have alleviating
315 effects, including its effect on L233 and L203 suffering from Cd^{II} toxicity (0.5 μM) or exposed
316 to a combination of Cd^{II} and Zn^{II}. The sizes of the alleviating effects of Mn were small and
317 mostly insufficient to rescue growth of these same strains at the next higher tested
318 concentration of 5 μM Cd, for instance (Table S9). In summary, we observed varied and
319 generally small combined effects of metals exacerbating or alleviating toxicity in keystone
320 strains, suggesting that combined effects are unlikely to cause major increases in metal
321 tolerance of strains compared to single metals as shown in Figure 1A.

322 **2.5 Phylogeny at the Genus Level Explains Most of the Variations in Metal Tolerance**
323 **Profiles**

324 Next, we examined metal tolerance profiles in relation to the phylogeny of *At*-LSPHERE
325 strains. *Actinobacteria* were significantly depleted by Cd concentrations of ≥ 15 μM and
326 enriched among the strains that continued to grow at ≥ 0.2 mM Cu and ≥ 0.4 mM Zn, when
327 compared to other classes (Figure 3). Relative to other classes, Gammaproteobacteria were
328 enriched at high levels of ≥ 2.5 mM arsenite. Hierarchical clustering of MPCs identified 10
329 distinct clusters of bacterial strains sharing similar metal(loid) tolerance profiles (Figure 4).
330 Cluster I comprised three strains, L92-*Methylobacterium*, L396-*Bradyrhizobium*, and L401-
331 *Bradyrhizobium* (all α-Proteobacteria), which were highly tolerant to multiple metals but not
332 to the metalloid arsenite. These strains were the most Cd-tolerant (1.5 mM) and tolerated more
333 than twice the EC_{50} concentrations of Cu, Zn, and Mn (Figure 4, Data S1). Cluster II consisted
334 of five highly Zn- and Cu-tolerant strains. Strains highly tolerant to arsenite grouped in cluster
335 III, highly Mn-tolerant strains in cluster IV, and highly Mn-tolerant and Cu-sensitive strains in
336 cluster V. Cluster VI comprised highly to moderately Cu-tolerant strains, some of which were
337 also highly Cd-tolerant. Clusters VII and VIII contained strains with intermediate Cu tolerance,
338 whereby cluster VII contained arsenite-sensitive and cluster VIII contained moderately
339 arsenite-tolerant strains. The final two clusters, IX and X, grouped strains that were highly Cu-
340 sensitive and sensitive to most other metal(loid)s, with intermediate tolerance to arsenite in
341 cluster IX and sensitivity to arsenite in cluster X. Metal tolerance profiles were similar within
342 the genus *Rhizobium*, of which approximately 73% grouped in Cluster X, and 13% in clusters
343 V and IX, respectively. In contrast, the seven *Rhodococcus* strains were distributed into four

344 different clusters: one strain in cluster III, two strains in the neighboring cluster VII, three
345 strains in cluster VIII, with two directly next to one another and a third one further away, and
346 finally one strain in cluster X. Similarly, the nine *Pseudomonas* strains were spread across the
347 five clusters V and VII to X, whereby only two of them clustered next to one another in cluster
348 V. These patterns suggested that phylogenetic relationships account for only part of the
349 variation in metal tolerance profiles.

350 To obtain more quantitative information on the contribution of phylogeny to the variation in
351 metal tolerance we employed dimensionality reduction-based analyses. There were no major
352 differences between strains of different taxonomic classes according to a PCA of strain-wise
353 MPCs (Figure S6A), and a constrained principal coordinate analysis (CPCoA) constrained by
354 class explained only 6% of the variance (Figure S6B; $p < 0.05$). By contrast, CPCoA attributed
355 42% of the variance to genus (Figure S6C; constrained by genus, $p < 0.001$). In agreement with
356 this, a representation of metal tolerances on a phylogenetic tree based on 16S rRNA DNA
357 sequences (Bai et al. 2015) suggested that closely related strains mostly exhibited similar metal
358 tolerance profiles (Figure 5). For example, *Methylobacterium* strains L90, L92, L119, L121,
359 L122, and L123 were highly Cd tolerant, and *Methylobacterium* L90, L92, and L122 were Cu-
360 and Zn-tolerant (Figure 5). Similarly, all *Bacillus* strains were sensitive to Cd and Cu, and all
361 *Rhizobium* strains (Alphaproteobacteria) were sensitive to Cu and Zn. In summary, metal(loid)
362 tolerances partially followed phylogenetic relationships, most prominently at the genus level,
363 suggesting that the remaining phenotypic variation among *At*-LSPHERE strains reflects recent
364 evolutionary divergence.

365 **2.6 Genetic basis of differential metal tolerances among bacterial strains**

366 We investigated the degree to which molecular mechanisms that were previously characterized
367 in bacteria can explain between-strain variation in metal tolerances. First, we conducted a PCA
368 of strain-wise MPC for Cd and the orthologs of genes described in the literature to increase Cd
369 tolerance that were present in the genome of each strain (Figure 6A). PC 1 clustered the classes
370 *Actinobacteria* and *Bacilli*, which were comparably Cd-sensitive (see Figures 3 and 5), together
371 towards one side, but left the other classes scattered across. PC loadings suggested a relation
372 between enhanced Cd tolerance and the presence of *czcA, B, C, D*, *smtA*, and *tolC*, of *zntA* for
373 PC1 only, as well as the absence of *zntR* and *cadC..smtB* (Figure 6A). Beyond the identity of
374 Cd tolerance genes, their gene dosage (or copy number) in a given genome could be expected
375 to scale with strain-level Cd tolerance. A Kendall's rank correlation analysis of the gene score,

376 which we calculated as the cumulative number of Cd tolerance-related genes and gene copies
377 present in the genome, and Cd MPC showed a significant correlation ($\tau = 0.31$, $p < 3.5 \times 10^{-9}$;
378 Figure 6B).

379 Subsequently, we addressed more generally whether differences in genomic content of known
380 bacterial metal tolerance genes are explained by phylogeny. For this, 100 known metal(loid)-
381 related genes (Data S2) were employed to carry out a CPCoA, constrained by class, which
382 indicated that 22% of the presence/absence genetic variation for metal tolerance-related genes
383 was explained by class ($p \leq 0.001$). Genus explained 63% of the genetic variation according to
384 CPCoA (constrained by genus, $p \leq 0.001$) (Figure S7A-C). These proportions further
385 highlighted the importance of genus-level taxonomy, consistent with the pattern observed for
386 phenotypic variation in metal tolerances (Figure S6). A higher proportion of genetic variation
387 than of phenotypic variation explained by genus (63% vs. 42% as reported in section 2.5) is
388 consistent with contributions of as yet unidentified genes to metal tolerance, which we would
389 expect to reduce the correspondence between known gene content and tolerance phenotype.

390 To test the effect of each gene on metal(loid) tolerances, bacterial strains were split into two
391 groups for each of the known metal(loid)-tolerance-related genes: one group in which the gene
392 of interest (GoI) was present in the genome and one group lacking the GoI (Data S3 and S4).
393 For each metal(loid), we then tested for significant differences between the median MPCs
394 calculated for the two groups (Wilcox rank-sum test, *p*-values adjusted with Holm-Bonferroni
395 correction). This approach identified a total of 51 genes which were significantly associated
396 with tolerance to one or more metal(loid)s: 21 genes (41%) for Cd, 10 for Cu (20%), 15 (29%)
397 for Zn, none for As^{III}, 20 (39%) for Mn, and 9 (18%) for As^{V} tolerance (Table S10, Data S4).
398 Among these, we detected a negative effect on Cd tolerance for *cadC..smtB* and positive effects
399 for *czcA, czcB, czcC, tolC* and *zntA* in agreement with Figure 6A, as well as additionally a
400 negative effect for *znuA* and positive effects for *zur* and *mdtA*, with the highest statistical
401 significances for *czcA*, *czcB*, *mdtA* and *tolC* (Data S4; Figure 7, $p_{adj} < 0.005$). Conversely, the
402 presence of *comB*, *cmtA*, and *smtB* each decreased the median MPC of Cd by a factor of 40,
403 and *csoR* decreased it by a factor of four. In addition to genes previously implicated in bacterial
404 Cd tolerance, our analysis identified *arsC1..arsC*, *arsH*, *cusB..silB*, *mdtA*, *mdtB*, and *mdtC* and
405 *zur* as candidate genes for increasing Cd tolerance. *Actinobacteria* and *Bacilli* of the *At*-
406 LSPHERE collection were characterized by an overall lack of Cd tolerance genes and the
407 presence of Cd-sensitizing genes, consistent with their Cd sensitivity (Figure 7, see Figures 3

408 to 5 and 6A). Out of all bacterial strains, the genomes of the four most Cd-sensitive strains
409 (L454, L172, L263, and L406) contained no or only few metal(loid)-related genes associated
410 with Cd tolerance, and genes related to Cd sensitivity were present in the genomes of three of
411 them (L172, L263, and L406; Figure 7). By contrast, the genomes of the most highly Cd-
412 tolerant strains contained comparably more Cd tolerance-increasing genes and few or no Cd-
413 sensitizing genes. The genome of strain L92-*Methylobacterium,* one of the two most highly
414 Cd-tolerant strains, was an exception to this pattern, containing only three known Cd tolerance-
415 increasing genes, *czcA, czcB* and *zntA*. Taken together, these results support roles in the leaf
416 phyllosphere for Cd tolerance genes previously characterized in bacterial model systems,
417 implicate additional metal(loid)-related genes in Cd tolerance, and suggest further
418 contributions to metal(loid) tolerances from previously uncharacterized or poorly annotated
419 genes.
420

421 # 3. Discussion

422 **3.1 Metal tolerances of individual strains and their relevance for bacterial community**
423 **composition in the leaf endosphere**

424 Our results support the conclusion that the levels of Zn and Cd, and possibly also of other
425 metal(loid)s, in the leaf apoplast contribute to shaping bacterial community composition in the
426 leaf endosphere of *A. thaliana* by eliminating or attenuating the growth of sensitive bacterial
427 genotypes. First, we observed marked overall differences in the degrees of tolerance to Zn and
428 Cd between the bacterial strain collection from the phyllosphere and the collection from
429 unplanted soil (Figure 1, Table 1). This suggests an enrichment of strains exhibiting elevated
430 tolerance to these metals among in the *At*-LSPHERE collection by comparison to the collection
431 from unplanted soil. Second, Zn and Cd concentrations in the leaf apoplastic fluid (AF) of soil-
432 grown Arabidopsis plants closely approached the metal concentrations that were toxic to metal-
433 sensitive bacterial strains of the *At*-LSPHERE collection in solid R2A media (Figures 1 and
434 S4, Table S5). In addition, Cd, Mn and Zn were enriched in AF compared to their
435 concentrations in bulk leaves. Third, two keystone strains (Carlström et al. 2019), L233-
436 *Rhodococcus* and L203-*Microbacterium*, were among the most highly Cd-sensitive strains
437 (Figures 2, and S5), implying the potential for pronounced secondary effects of Cd toxicity on
438 overall species composition in the leaf endosphere. Finally, a set of exemplary tests conducted
439 by us suggested that between-strain and between-metal interactions had no, or only few and

440 mostly small, reproducible effects alleviating Zn or Cd toxicity (Figures 1 and 2, S2 and S3,
441 Tables S8 and S9).

442 Our study has some limitations that should be considered when interpreting these conclusions.
443 There are some limitations affecting these conclusions from our study. While partly shared soil
444 environments of origin support the comparability of the bacterial collections (Bai et al. 2015),
445 the number of strains was considerably smaller in the soil collection than in the *At*-LSPHERE
446 collection, thus potentially decreasing the precision of the values summarizing
447 metal(loid)tolerances across soil bacterial strains (Figure 1). Relating metal concentrations in
448 leaf AF to those in solid or liquid bacterial growth media fundamentally remains an
449 extrapolation. Considerable proportions of the total metal concentrations accessible to and
450 measured in AF, as well as those measured in R2A media, are present in chelated form in
451 solution, within precipitates or bound to the surfaces of solids. Yet, the degree of Cd and Zn
452 toxicity to bacteria depends on the concentrations of their free aqueous divalent cations. In
453 addition to this, the levels of other solutes can strongly influence metal toxicity either directly
454 or indirectly. Importantly, other divalent cations compete with toxic metal cations for bacterial
455 uptake, and the levels of bioavailable nutrients, such as phosphate, sulfur, iron and manganese,
456 can alleviate metal toxicity inside bacterial cells. The overall elemental composition of solid
457 R2A media (*ca*. 5-fold Fe, 10% Ca, 30% Mg, 20% K, 6-fold S, and 2.6-fold P, compared to
458 AF) suggested that bacterial metal toxicities are broadly comparable between the two matrices
459 (Table S5). The agar polysaccharide in solid R2A medium contributes a macromolecular
460 matrix of metal cation binding sites, similar to the cell walls of Arabidopsis which interact with
461 the AF *in vivo*. Agar also contributes substantial quantities of contaminant Ca^{2+} and Mg^{2+}
462 cations capable of competing with Cd^{2+} and Zn^{2+}, compared to liquid R2A media (Table S3).
463 Thus, unsurprisingly, bacteria generally tolerated higher Cd concentrations in solid than in
464 liquid R2A medium (≥ 16-fold difference for L262 and the intermediate SynCom, > 10-fold
465 for L203 and L233; compare Fig. 1C with Figure S2, Fig. 2A with Suppl. Fig. S5).

466 We expect the composition of leaf AF to be highly dynamic, which must be kept in mind when
467 comparing with the metal concentrations in our bacterial tolerance assays. In addition to the
468 concentrations of free metal cations and other contributing factors outlined above, a pH
469 decrease (Geilfus 2017; Geilfus et al. 2020) and a more oxidized redox state can directly
470 enhance metal toxicity in AF by decreasing the proportion of metal cations in complexed or
471 bound from, thereby increasing the bioavailable fraction of free aqueous metal cations.

472 Importantly, in response to infection by the necrotrophic fungus *Plectosphaerella cucumerina*,
473 Arabidopsis accumulated Zn^{2+} in the leaf apoplast dependent on the Zn^{2+}/Cd^{2+} efflux pump-
474 encoding genes *AtHMA2* and *AtHMA4* (Escudero et al. 2022). Microbe-induced fluxes of metal
475 cations across the plasma membrane of plant cells may be more widespread than is currently
476 recognized. Interpreting the differences in overall metal tolerances of the *At*-LSHERE
477 collection compared to soil bacterial communities as an outcome of selective strain enrichment
478 would imply that in phyllosphere bacterial communities even the mildest Zn and Cd toxicities
479 are ecologically relevant (compare EC_5 in Table 1). We observed the largest relative
480 differences between *At*-LSPHERE and soil bacterial Zn and Cd tolerances for EC_{95} (Table 1).
481 One possible interpretation of this observation is that severe metal toxicities are ecologically
482 highly important for Zn^{II} (corresponding to the degree of toxicity inflicted by 0.66 to 11 mM
483 Zn in solid R2A medium), Cd^{II} (0.054 to 0.56 mM Cd) and possibly also Cu^{II} (1.4 to 1.6 mM
484 Cu^{II}).

485 In contrast to Zn, Cd has no known nutritional role in Arabidopsis, raising the question of
486 acquisition and partitioning of Cd by plants in conjunction with the possible biological role in
487 plant-microbe interactions suggested by our results. In addition to HMA2 and HMA4, and
488 among other characterized membrane transporters (Sterckeman and Thomine 2020), Cd^{2+} is a
489 secondary substrate of the high-affinity root Fe^{2+} uptake systems IRT1 of Arabidopsis and
490 RIT1 of pea (Cohen, Garvin, and Kochian 2004; Connolly, Fett, and Guerinot 2002; Vert et al.
491 2002). In the Zn- and Cd-hyperaccumulating species *Arabidopsis halleri*, extremely high
492 concentrations of 3 to 54 mg g^{-1} Zn and 0.1 to 3.6 mg g^{-1} Cd in bulk leaf dry biomass are
493 thought to function as elemental defenses against biotic stress (Kazemi-Dinan et al. 2014; Stein
494 et al. 2017; Hörger, Fones, and Preston 2013). Maximal Zn and Cd concentrations in leaves of
495 healthy *A. thaliana* plants are less than 10% by comparison, but this does not preclude the
496 possibility of a highly localized accumulation of Zn or Cd to levels that can be toxic for
497 bacteria. Much higher bacterial toxicity of Cd compared to Zn (Table 1), as well as the poor
498 correlation between Cd and Zn tolerance among *At*-LSPHERE strains (Figure 4), argue against
499 the possibility that our findings could merely be a consequence of the general similarity
500 between the chemical properties of Cd and Zn.

501 For metal(loid)s other than Zn and Cd, there was substantially less evidence for a role in
502 shaping phyllosphere microbial communities. Cu^{II} concentrations in AF were far below Cu^{II}
503 levels toxic for *At*-LSPHERE bacteria on agar-solidified media, and *At*-LSPHERE bacteria

504 were not generally more Cu^{II}-tolerant than soil bacteria (Figure 1). Cd toxicity to the keystone
505 strains L233-*Rhodococcus* and L262-*Rhizobium* was potentiated by the additional presence of
506 Cu^{II} only at a high concentration of 100 µM in liquid R2A medium (Figure 2). However, some
507 existing knowledge supports that Cu could be relevant in plant-microbe interactions. Human
508 macrophages mediate the local accumulation of Cu ions in the phagolysosome to kill pathogens
509 (Achard et al. 2012; White et al. 2009; Samanovic et al. 2012). Transcript profiling revealed
510 that several copper-related genes were upregulated in *A. thaliana* leaves in response to the
511 strain *Methylobacterium extorquens* PA1 (Vogel et al. 2016), and the treatment of Arabidopsis
512 with Cu was reported to enhance its immunity against *Pseudomonas syringae* pv *tomato*
513 DC3000, for example (Xia et al. 2026). The strongest biotoxic effects of Cu generally result
514 from redox cycling between oxidized Cu^{II} and reduced Cu^{I}, and from exposure to Cu^{I}
515 (Samanovic et al. 2012). Plasma membrane-localized $gp91^{phox}$ NADPH oxidases, such as the
516 superoxide-producing *At*rbohD and *At*rbohF as well as the Cu^{II} chelate reductases *At*FRO4 and
517 *At*FRO5, could contribute to redox cycling of Cu in a manner analogous to their proposed role
518 in human immune cells (Torres, Dangl, and Jones 2002; Nathan and Shiloh 2000) and to the
519 reduction of extracellular Cu^{II} to Cu^{I} (Bernal et al. 2012). Indeed, *AtrbohD* is important for the
520 maintenance of microbiota in leaves of *A. thaliana* (Pfeilmeier et al. 2021), but a relationship
521 with Cu was not reported. Total As was below our detection limits in AWF, and bacteria
522 seemed to be comparably tolerant to arsenite (As^{III}) and arsenate (As^{V}) on solid R2A medium.
523 Organo-arsenicals, which can be far more toxic than inorganic forms of As, warrant further
524 investigation, given that *A. thaliana* can take up dimethylarsenate and convert it into
525 dimethylmonothioarsenate- and dimethyldithioarsenate, for example (Colina Blanco et al.
526 2023). For Mn and As^{III}, only EC_5 values were higher in the *At*-LSPHERE than in the soil
527 bacterial collection, implying a possible ecological relevance associated with mildly toxic
528 concentrations in AF (Table 1), which will require further work. The finding that Mn^{II}
529 alleviated Cd^{II} toxicity in keystone strain L203-*Microbacterium* in liquid R2A media may be
530 related to this (Figure 2).

531 To date, the information available from previous metal(loid) tolerance screens of bacterial
532 strain collections is limited. Much of the available information is from single bacteria
533 hypothesized to exhibit enhanced metal(loid) tolerance (Zhao et al. 2015; Tada and Inoue
534 2000), and from multiple strains collected in environments characterized by high levels of
535 abiotic stress or heavy metals (Abou-Shanab, van Berkum, and Angle 2007; Nieto, Ventosa,
536 and Ruiz-Berraquero 1987). Overall, these studies concur with our results regarding the

537 comparably high toxicity of Cd and the overall narrow concentration range for Cu^{II} (see Table
538 1, Figure 1). Although *Actinobacteria* were the least Cd-tolerant among *At*-LSPHERE strains,
539 a study of heavy metal-tolerant *Actinobacteria* identified strains able to tolerate Cd and Cu
540 concentrations of up to 100 mM, i.e., about 70- and 100-fold higher concentrations than the
541 most tolerant strains of the *At*-LSPHERE collection (Amoroso et al. 1998). Across these
542 previous studies, natural variation in bacterial metal tolerances is very large, and the
543 environment of bacterial origin appears to be more influential than their phylogeny. Metal
544 tolerances of *At*-LSPHERE strains were mostly lower than those reported in bacteria
545 originating from metal-rich environments, with some remaining uncertainty given the diversity
546 of media and designs among tolerance assays used.

547 **3.2 Relationship of metal(loid) tolerance with phylogeny and the gene content of bacterial**
548 **genomes**

549 Phylogenetically closely related bacteria tended to exhibit similar metal tolerance profiles, and
550 our results supported a genetic basis of differential metal tolerance profiles (Figures 5 to 7).
551 However, there were some notable exceptions of closely related bacteria with contrasting metal
552 tolerance profiles (Figure 2) and of bacterial strains for which metal tolerance phenotypes
553 deviated from expectations based on the metal tolerance genes present in the genome. For
554 instance, only a few of the genes related to Cd tolerance were present in the genome of L92-
555 *Methylobacterium*, which was among the three most highly Cd-tolerant strains (Figure 7). The
556 functions of identically annotated genes may differ between bacterial strains, and of the genes
557 contributing to bacterial metal tolerances some are likely to remain unidentified, for example
558 in the Cd-tolerant strains L337- and L137-*Arthrobacter*.

559 We identified some candidate genes in *At*-LSPHERE strains among the genes annotated as
560 metal(loid)-related based on previous work in bacterial models (Figures 7, Table S10). Of the
561 genes strongly implicated in Cd tolerance in the *At*-LSPHERE collection, the *czc* and *znt*
562 operons are well-known (Figures 6 and 7, Table S10, Data S4). The CzcCBA efflux system of
563 *Ralstonia metallidurans* pumps Cd out of cells (Nies et al. 1989; Nies and Silver 1989; Nies
564 1992b) for Cd resistance (Silver and Walderhaug 1992; Nies 1992a), supported by a virtual
565 model of *R. metallidurans* (Legatzki et al. 2003). Bacterial ZntA Zn/Cd/Pb-transporting P-type
566 ATPase proteins often function in Zn detoxification and are also relevant for Cd resistance
567 (Rensing, Mitra, and Rosen 1997; Singh et al. 1999; Outten, Outten, and O'Halloran 1999;
568 Beard et al. 1997; Choudhury and Srivastava 2001; Chaoprasid et al. 2015). A low

569 concentration of Cd (50 µM) completely inhibited growth of an *Agrobacterium tumefaciens*
570 C58 loss-of-function *zntA* mutant (Chaoprasid et al. 2015). Surprisingly, we did not identify
571 the gene encoding the known regulator of *zntA*, *zntR* (Table S10), and its presence even
572 appeared to be inversely related to Cd tolerance (Figure 6).

573 In addition to these well described Cd tolerance mechanisms, our data implicated Resistance-
574 Nodulation-Division (RND) type multidrug efflux pump component-encoding *mdtA*, *B*, and *C*
575 in Cd tolerance of *At*-LSPHERE bacteria. In *Escherichia coli*, periplasmic MdtA connects the
576 inner membrane efflux pump MdtBC to the outer membrane channel TolC to confer antibiotic
577 resistance (Nagakubo et al. 2002; Nishino, Nikaido, and Yamaguchi 2007; Kim, Nagore, and
578 Nikaido 2010). The fourth gene of the *mdtABCD* operon *mdtD* encodes a putative transporter
579 MdtD, which is also involved in antibiotic resistance and can promote the efflux of citrate, later
580 renamed iron-citrate efflux Transporter IceT in *Salmonella typhimurium* (Frawley et al. 2013).
581 A knockout of *tolC* in *E. coli* resulted in Cd hypersensivity (Achard-Joris et al. 2005).
582 Moreover, mRNA of genes encoding the AcrAB-TolC efflux pump (*acrB* and *tolC*) were
583 upregulated in Cd-adapted *Salmonella* Typhi Ty2 cells (Kaur et al. 2021). The MdtABC system
584 was implicated in Zn and Cu tolerance in *Salmonella enterica* (Nishino, Nikaido, and
585 Yamaguchi 2007). Supporting the *in planta* relevance of RND-type efflux systems, an RND
586 family efflux transporter MFP subunit (Mext_2832) was detected in the *in planta* proteome of
587 *M. extorquens* PA1 (Müller, Schubert, et al. 2016), and efflux systems including CzcABC
588 family RND transporters were among the proteins induced during phyllosphere colonization
589 in *Rhizobium* L68 and *Sphingomonas* L257 (Hemmerle et al. 2022).

590 Our results implicated genes with well-characterized roles in As tolerance, *arsC1..arsC* and
591 *arsH*, in Cd tolerance of *At*-LSPHERE strains (Figures 6 and 7, Table S10, Data S4). Among
592 three different KO identifiers linked to *arsC* (*arsC1..arsC*, K00537; *arsC2..arsC*; K03741,
593 *arsC*, K18701; Data S4), only *arsC1..arsC* (*arsC1*), described as arsenate reductase that uses
594 glutathione as a cofactor (glutaredoxin) in the KEGG database, showed a positive effect on Cd
595 tolerance. Dhankher et al. (2003) reported that bacterial *arsC1* conferred Cd tolerance to *E.*
596 *coli*, and to *A. thaliana* and *Nicotiana tabacum* plants, but the underlying mechanism remains
597 unidentified. The second Cd tolerance candidate gene in the *ars* operon, *arsH* was described
598 as a methylarsenite oxidase that can form the less toxic methylarsenate (Yang and Rosen 2016)
599 and as an H_2O_2-producing enzyme that can alleviate oxidative stress in *Synechocystis* PCC
600 6803 (Lopez-Maury, Florencio, and Reyes 2003). In *Pseudomonas chenduensis* strain MBR,

601 *arsH* transcript levels were upregulated under Cd toxicity (Li et al. 2020). There is no published
602 information on roles in Cd tolerance for the two remaining Cd tolerance candidate genes, *cusB*
603 (annotated to encode a component of a Cu^{+} detoxification system), and *zur* (encoding a Zn
604 sensor mediating the transcriptional repression of genes encoding high-affinity Zn uptake
605 systems in its Zn^{2+}-bound form). Effective repression of Zn^{2+} uptake may help to decrease
606 inadvertent uptake of Cd^{2+} cations when they are abundant. We detected no effect for
607 *cadC..smtB*, which was previously implicated in bacterial Cd tolerance (Endo and Silver 1995).

608 Future work should test further the hypothesis supported by our results that apoplastic Zn and
609 Cd contribute to the structuring of bacterial communities in the leaf endosphere of *A. thaliana*,
610 as well as investigate the roles of physiologically relevant chemical forms of Cu and As that
611 could not be tested here. What currently remains limiting is the lack of cell biology tools
612 capable of quantitatively monitoring the dynamics of apoplastic free metal cation
613 concentrations and of genetic tools for changing these without affecting other aspects of plant
614 metal homeostasis that could have indirect effects on microbial performance. In the future,
615 exclusion of epiphytic bacteria may facilitate the analysis of interactions between the plant host
616 and bacteria in the leaf endosphere (Chen et al. 2020). Finally, future functional studies can
617 target metal(loid) tolerance candidate genes identified here in the published genomes of *At*-
618 LSPHERE bacteria.

619 4. Material and Methods

620 4.1 Plant Material and Growth Conditions

621 *Arabidopsis thaliana* (L.) Heynh., accession Columbia (Col-0), wild-type plants were sown on
622 commercially available greenhouse soil (Balster Einheitserdewerk, Fröndenberg, Germany) in
623 10 cm x 10 cm x 11 cm square pots (~ 100 seeds per pot) and watered once with Previcur
624 Energy (Bayer CropScience, Monheim, Germany) against fungi, followed by stratification at
625 4°C in darkness for 2 d. Subsequently, plants were transferred into a growth chamber (CLF
626 Plant Climatics, Wertingen, Germany) and grown in short-day conditions (145 µmol m^{-2} s^{-1}
627 and 22°C for 8 h, dark period at 18°C for 16 h). Two weeks later, equal-sized seedlings were
628 transferred into fresh pots (one plant per pot, 0.7 L greenhouse soil, or a mix of natural soil
629 from Bad Gottleuba, 50°50'45.7" N 13°59'43.1" E, with sand and greenhouse soil, at 35 + 15
630 + 50 volume parts, respectively), and covered with a clear plastic humidity dome for one week.
631 Plants were fertilized once every 14 d (0.3% (v/v) Wuxal Super 8-8-6, Hauert MANNA

632 Düngewerk GmbH, Nürnberg, Germany), watered with a suspension of *Bacillus thuringiensis*
633 *israelensis* (Neudomück, W. Neudorff GmbH KG, Emmerthal, Germany) against fungus gnats
634 once a week, and cultivated in individual pots for seven to eight weeks in total.

635 **4.2 Isolation of Apoplastic Wash Fluid from Leaves of *A. thaliana***

636 All handling of plant tissues was conducted using plastic tweezers. For each sample, leaves of
637 ≥ 75% full-grown length that appeared healthy and unscathed were cut off at the petiole using
638 a razor blade, pooled from two *A. thaliana* plants, rinsed in ultrapure water, blotted dry, and
639 weighed. The isolation of apoplastic wash fluid was carried out according to O'Leary et al.
640 (2014), with modifications. Leaves were immersed in an infiltration fluid (IF) of either
641 ultrapure water or 100 µM EDTA (pH 7.2) inside a 1-L side arm vacuum flask containing 1 L
642 of IF and covered by a plastic mesh cover that was weighed down by a glass rod placed on top
643 of the mesh. We conducted three cycles of vacuum infiltration at 30 mbar for 3 min followed
644 by the release of the vacuum over a period of 3 min. After recovering the leaves and blotting
645 them dry gently with soft tissue paper, five to eight leaves of one sample were placed next to
646 one another on a 10 cm x 10 cm segment of Parafilm ("M" strips; PECHINEY PLASTIC
647 PACKAGING, Chicago, United States of America), rolled gently around the outer surface of
648 5-mL pipette tips, and the arrangements were then placed tip-down into 50-mL polypropylene
649 tubes. This procedure was repeated until all leaves had been processed. Apoplastic wash fluid
650 (AWF) was extracted by centrifuging in a swinging bucket rotor at 1,000x*g* and 4°C for 15
651 minutes, followed by measuring the volume of each obtained AWF sample and weighing the
652 remaining extracted leaves. Leaf biomass was used as an information to track possible
653 differences in hydration status between plants and experiments, but was not used in any
654 calculations. The recovered AWF was transferred into 1.5-mL tubes, centrifuged at 15,000x*g*
655 for 5 min, and the supernatant transferred into a fresh 1.5-mL tube and stored at -80°C. To
656 estimate the concentrations of solutes in apoplastic fluid (AF) *in vivo* from concentrations
657 measured in AWF samples, we experimentally determined a dilution factor for the AF in the
658 AWF (2.35; n = 4) in one experiment, as described in O'Leary et al. (2014). To test for
659 cytoplasmic contamination, glucose-6-phosphate dehydrogenase (G6PDH) activity was
660 quantified in one initial experiment using a commercially available assay kit (Sigma-Aldrich)
661 according to the user manual (Data S5). Compared to a PCA of ionomic profiles of AF (Figure
662 S4; see Methods below), G6PDH activity was a far less sensitive marker for the detection of
663 cytoplasmic contamination (Data S5). To identify the effects of cytosolic contamination on

664 AWF composition, we intentionally damaged leaf samples (in duplicate) using both IF
665 solutions in each experiment. For weak simulated damage, we released the vacuum faster. For
666 intermediate simulated damage, we additionally handled the infiltrated leaves harshly. For
667 strong simulated damage, we additionally pressed the leaves against the 5-mL pipette tips. In
668 each experiment, IF was sampled from the vacuum flasks following the removal of the leaves
669 after infiltration to quantify baseline contamination originating from the leaf surface, as well
670 as from the materials and solutions used.

671 **4.3 Multi-Element Analysis**

672 To estimate the elemental composition of leaf AF of *A. thaliana,* AWF was dried in 1.5-mL
673 polypropylene tubes at 60°C for 7 d, and subsequently acid-digested by adding 500 µL 65%
674 (w/w) HNO_3 and incubating RT overnight, then heating to 60°C for 1 h, 80°C for 1 h and 100°C
675 for 1 h, with automated mixing at 300 rpm for 30 s every 5 min (Thermomixer Comfort,
676 Eppendorf SE, Hamburg, Germany). Digests were transferred to 15 mL polypropylene tubes,
677 together with an additional rinse of the 1.5-mL tubes with 500 µL 65% (w/w) HNO_3, and
678 samples were filled up to a final volume of 5 mL with ultrapure water after cooling. For multi-
679 element analysis of leaves, they were placed into 4.4 × 8 cm paper bags and dried at 60°C for
680 7 d and then equilibrated at room temperature for ≥ 3 d. Dried leaves were homogenized in
681 1.5-mL tubes with 3 to 5 acid-washed ceramic beads at 30 s^{-1} for 30 s (Retsch MM300,
682 RETSCH GmbH, Haan, Germany). Aliquots of approximately 20 mg dried leaf powder were
683 weighed into perfluoroalkoxy alkane (PFA) vessels and digested in 3 mL 65% (w/w) HNO_3
684 using microwave-assisted digestion (1600 W, ramp time 20 min, hold time 15 min (190°C))
685 ($MARSX_{PRESS,}$ CEM Corporation, Matthews, USA). After cooling down to RT in ambient air,
686 digests were transferred into 15-mL polypropylene tubes and filled up to a final volume of 5
687 mL with ultrapure water. For multi-element analyses of liquid R2A media, 50-mL samples
688 were dried in PFA tubes at 100°C and subsequently digested as described for leaf material. To
689 analyze the agar used in solid R2A media, aliquots of around 120 mg were weighed into 15-
690 mL polypropylene tubes, incubated in 2 mL 65% (w/w) HNO_3 at RT overnight and filled up
691 to a total volume of 10 mL with ultrapure water. Multi-element analysis was conducted using
692 Inductively Coupled Plasma-Optical Emission Spectrometry (ICP-OES) in an iCAPDuo 6500
693 instrument (Thermo Fisher, Dreieich, Germany). Calibration was done using a blank and a
694 series of five multielement standards that were manually pipetted from single- element standard
695 solutions for 13 (AWF from experiments on greenhouse soil) or 16 (AWF from experiments

696 on the natural soil mix) elements commonly detected in Arabidopsis and expected to be present
697 in the apoplast, and 17 elements for analyses of bulk leaves (AAS Standards; Bernd Kraft,
698 Duisburg, Germany). The precision of measurements was validated by measuring a sample
699 blank and an intermediate calibration standard, as well as for the analysis of leaves additionally
700 a certified reference material (Virginia tobacco leaves, INCT-PVTL 6; Institute of Nuclear
701 Chemistry and Technology, Warsaw, Poland) and an *A. thaliana* lab-internal reference
702 material. Soil total and HCl-extractable fractions were prepared and analyzed as described
703 (Stein et al. 2017).

704 **4.4 Media Preparation**

705 Media were prepared as described by Bai et al. (2015) with the following changes: Before
706 pouring plates, solid R2A media were cooled to 44°C and supplemented with metal or
707 metalloid from 100 mM or 1 M stock solutions to final concentrations as indicated in Table
708 S2. All metal and metalloid stock solutions were sterile-filtered after preparation, using a 50
709 mL syringe (TERUMO EUROPE N.V., Leuven. Belgium) and a sterile syringe filter (Filtropur
710 S (0.2 µm), SARSTEDT AG & Co. KG, Nürmbrecht, Germany), and stored at room
711 temperature or 4°C. For the arsenate concentration series including the control, low-phosphate
712 R2A medium was used (Table S1). Metal tolerance screening was conducted on square (120 x
713 120 x 17 mm) plates. Liquid media was prepared as described above excluding the addition of
714 agar.
715

716 **4.5 High-Throughput Metal Tolerance Screening**

717 Each of the 224 isolates of the *A. thaliana* phyllosphere (*At*-LSPHERE; Bai et al.
718 2015)collection was cultivated in 3 mL liquid R2A medium containing methanol (0.5% v/v) in
719 darkness at room temperature, with continuous shaking (300 rpm), for 2 to 3 d. Saturated
720 cultures were mixed 1:1 (vol:vol) with sterile-filtered 70% (v/v) glycerol in ultrapure water
721 and stored in 96-well plates at -80°C. Stocks in 96-well plates were defrosted and screened
722 under sterile conditions on solidified R2A media using a sterilized 96-pin microplate replicator
723 (Boekel Scientific, Feasterville, USA). The inoculated plates were incubated at RT in the dark
724 for up to 20 d. Photos were taken after 10 and 20 days of cultivation. Growth was scored based
725 on the photos. For metal screening, nine independent experiments were performed in total.
726 Three independent experiments (repeats) were conducted for each metal(loid) series, each
727 consisting of a control of unamended medium and six different concentrations (Table S2).

728 When needed, further experiments were conducted including additional metal(loid)
729 concentrations to estimate growth parameters (Table S2, see data analysis below). Surviving
730 strains were scored after 10 d of cultivation, and their number normalized to that on the
731 unamended control medium.
732

733 **4.6 Assessment of Tolerances of Single Strains in Liquid Medium**

734 The four keystone strains L203-*Microbacterium*, L231-*Sphingomonas*, L233-*Rhodococcus,*
735 and L262-*Rhizobium* (Carlström et al. 2019) were cultivated on round petri plates containing
736 agar-solidified R2A medium (60 x 15 mm) at RT for one week. Subsequently, single colonies
737 were transferred into 3 mL of liquid R2A medium and cultivated at RT for 1 to 2 d. Each strain
738 was diluted with sterile liquid R2A medium to an OD_{600} of 0.2 (SYNERGY HTX multi-mode
739 reader, BioTek Instruments GmbH, Bad Friedrichshall, Germany), mixed 1:1 (vol:vol) with
740 70% (v/v) sterile-filtered glycerol and stored at -80°C. For the quantification of metal
741 tolerances based on growth curves, five µL of each stock bacterial suspension, or of a 1:1
742 (vol:vol) mix of liquid R2A medium and sterilized 70% (v/v) glycerol in ultrapure water for
743 blanks, were added per well containing 195 µL liquid R2A media with or without (control)
744 metal supplementation (three independent experiments, 5 technical replicates per experiment)
745 in a 96-well plate. Bacterial strains were cultivated in darkness at 22 to 28°C for 24 h (Cd only,
746 Figure S5) and 48 h (combined metal toxicities, Figure 2B and C, Table S8 and S9), with hourly
747 OD_{600} measurements (SYNERGY HTX multi-mode reader) preceded by horizontal shaking at
748 200 rpm for 5 min.

749 **4.7 Experiments with Synthetic Communities**

750 We designed three synthetic communities (SynComs) consisting of 10 strains with low,
751 intermediate, and high Cd tolerance, respectively, which matched the phylogenetic profile of
752 the full *At*-LSPHERE collection as closely as possible (Figure S2 and S3). Strains were pre-
753 cultivated as described for single-strain tolerance quantification. For each SynCom, 100 µL per
754 strain of individual 1:1 (vol:vol) suspensions of the bacterial culture and 70% (v/v) sterile-
755 filtered glycerol were combined to obtain a final total volume of 1 mL, followed by storage of
756 both the SynComs and the single-strain pre-cultures at -80°C. To test for growth of the
757 SynComs and the constituent single strains on solid R2A media supplemented with a series of
758 Cd concentrations, 5-µL aliquots of each stock were spotted manually, and plates were
759 incubated in darkness at RT for 10 d. Cd tolerances of SynComs were quantified in liquid R2A

760 medium as described for the keystone strains above, with an OD_{600} measurement once every
761 30 minutes over a period of ≥ 20 h (5 independent experiments, with 6 technical replicates per
762 experiment).

763 **4.8 Data Analysis and Visualization**

764 All data was organized in Microsoft Excel (Microsoft Corporation, Redmond, USA) and
765 analyzed using the R computing language (version 4.3.0 (R_Core_Team 2023)) in the Rstudio
766 environment (version 2023.06.0.421 (Posit_team 2023)). Graphical abstracts, schemes, and
767 plot fine-tuning were carried out using Inkscape (version 1.2.2 (Inkscape_Project 2020)).

768 *Processing of data from metal(loid) tolerance screening of the At-LSPHERE strain collection*

769 Strains surviving on metal-amended solid R2A media were counted and normalized to the total
770 number of strains to calculate survival rates. The `GRfit()` function from the *GRmetrics*
771 package was used to obtain dose-response curves and to calculate various metrics. With a
772 modified `GRdrawDRC()` function and the *ggplot2* package, data were plotted alongside dose-
773 response curves ($f(x) = E_{inf}+(1-E_{inf})/(1+(x/EC_{50})^h)$) (Figure 1A & B). To calculate EC_n values
774 shown in Table 1, $EC_n = ((1+E_{inf})/((1-n/100)-E_{inf})\times EC_{50}^h-EC_{50}^h)^{1/h}$ was used (E_{inf} : proportion
775 of bacteria surviving an infinite metal concentration, set to 0 for calculating EC_n; EC_n:
776 metal(loid) concentration at which *n*% of the strains failed to grow; *h*: Hill coefficient of the
777 fitted curve; *x* the metal concentration in the medium [mM]; and *y* the proportion of surviving
778 strains [%]. pie plots were generated using the *ggplot2* and *tidyverse* packages from counts of
779 strains surviving at each specific metal(loid) condition were counted and normalizing by
780 phylogenetic class. Statistical significance*s* of depletion or enrichment of each class were
781 calculated using Fisher's exact test, Then, *p*-values were corrected for false discovery rates by
782 calculating *q*-values with the *qvalue* package.

783 Next, we calculated the strain-wise maximum permissive concentration (MPC) for each
784 metal(loid) as the median of three independent experiments based on our raw data. For those
785 bacterial strains and metal(loid)s for which MPCs were apparently below the lowest or above
786 the highest metal concentrations employed in our initial concentration series, we conducted
787 additional experiments including lower/higher metal concentrations as appropriate. To show
788 the metal tolerances of the keystone strains, spider charts were generated using Microsoft
789 Excel.

790 *Clustering of metal tolerance profiles and tests for relationships between metal tolerance and*
791 *phylogeny*

792 Medians of strain-wise MPC were converted to *z*-scores across isolates for each metal using
793 the `scale()` function. A Euclidean distance matrix was generated with the `dist()` function
794 for hierarchical clustering. Based on an agglomerative coefficient of 0.98 calculated using the
795 `agnes()` function from package *cluster*, Ward clustering was the best-fitting method.
796 Therefore, for clustering the `hclust()` function was used with the ward.D2 method. The
797 heatmap plot was generated with the `heatmap.2()` function from the *gplots* package, with a
798 customized dendrogram created with the *colorspace* (for color palette) and the *dendextend*
799 packages. Principal components (PCs) were calculated with the `prcomp()` function. To test
800 the significance of the PC analyses (PCA), the package *PCAtest* was used. Null distributions
801 for PCA statistics were generated using 999 random permutations, and sampling variance was
802 estimated based on 999 bootstrap replicates. Loading indices were used to evaluate the effect
803 of variables (loadings) to each PC. PCAs were plotted using the `ggbiplot()` function from
804 the package *ggbiplot* and the package *ggplot2*. For a constrained principal coordinate analysis
805 (CPCoA), the package *vegan* with the `capscale()` function was used. The analysis was
806 constrained either by class or by genus. Statistical significance of the ordinations and
807 confidence intervals for the variance were calculated by ANOVA-like permutation tests with
808 the `permutest()` and `anova.cca()` function with 99 permutations (Robbins et al. 2018).
809 Results were plotted with the `ggplot()` function from *ggplot2* package.
810 The phylogenetic tree was built using the 16s rRNA sequences published (Bai et al. 2015). All
811 206 sequences available for strains of the collection were downloaded from www.at-
812 sphere.com. To generate a tree, the sequences were aligned with `msa()` function from the *msa*
813 in R, followed by the computation of a distance matrix using the `msaConvert()` function
814 from the *msa* package and the `dist.alignment()` function from the *seqinr* package.
815 Finally, the tree was built with `bionj()` function from *ape* package. For each strain and
816 metal(loid), the MPC was normalized to the EC_{50} of the full *At*-LSPHERE collection (see Table
817 1), linked to the tree, and plotted using the *ggtree* and *ggfruit* packages.

818 *Processing of data from time-dependent growth curves in liquid media for Cd and combined*
819 *metal tolerances*

820 OD_{600} values were ln-transformed and plotted in R. To calculate doubling times during in Cd-
821 exposed cultures, the first observed Log phase of growth, the initial (Time T1, $\ln(OD_{600}1)$,)
822 and final (Time T2, $\ln(OD_{600}2)$) values were extracted using the *zoo* package and a linear
823 model, followed by the calculation of the growth rate $r = \ln(OD_{600}2/OD_{600}1) / (T2-T1)$ and the
824 doubling time $t_d = \ln(2)/r$ and plotting with R. To analyze tolerances in combined metal
825 treatments, the growth curves were fitted with generalized additive models with integrated
826 smoothness estimation. For growth detection, a threshold was established (six times the
827 standard deviation from all measurements during the initial 4 h of cultivation) and the average
828 timepoint calculated at which OD_{600} reached this threshold (significance testing by one-way
829 ANOVA with Tukey's multiple comparisons *post hoc* test). Visual changes of growth curves
830 (V), defined as noticeable alterations in the trajectory or shape of the growth curve indicating
831 an impairment relative to the control, were scored together with significant increases in the
832 time points of threshold crossing (T) and summarized (Table S8 and Table S9). Results were
833 visualized with the free and open-source vector graphics editor Inkscape.

834 *Analysis for associations between metal tolerance and the presence of metal(loid)-related*
835 *candidate genes in the genome*

836 Based on the available KEGG Orthology (KO) database annotations for the *At*-LSPHERE
837 collection (Bai et al. 2015) we identified genes that named any of the metal(loids) tested here
838 in the description. Only genes present in at least 8 strains were retained, resulting in a total of
839 100 genes analyzed further (Data S2). KEGG data were loaded from www.at-sphere.com to
840 analyze the presence/absence of genes (Data S3) in the genome of each strain of the *At*-
841 LSPHERE collection. The dataset was organized with the `pivot_longer()` function from
842 the *tidyr* package. For each metal(loid)- related gene, bacterial strains were split into two
843 groups, one group in which the gene of interest was present in the genome and one group
844 lacking the gene of interest. For each metal(loid), we tested for significant differences between
845 the median of strain-wise MPCs of the two groups employing a Wilcoxon rank-sum test with
846 Holm-Bonferroni corrections (p_{adj}, Data S4). Among the resulting gene-metal pairs, we then
847 selected the subset for which the median of at least one MPC differed significantly between
848 groups by a factor of ≥ 2 (Table S10). We visualized the genomic copy number of genes as a
849 circular heatmap, as described above for strain-wise MPCs. All 100 genes were used for a
850 Constrained Principal Component Analysis (CPCoA) on the presence/absence of genes. The
851 statistical significances of constraints and of axes were assessed using the function

852 `anova.cca()` from the *vegan* package to conduct an ANOVA-like permutation test for
853 distance-based redundancy analysis (Permutation test, 999 permutations).

854 To test for the correlation of Cd tolerance with the number of genes with expected functions in
855 Cd tolerance present in the genome, we conducted a PCA of presence/absence of these genes
856 together with the MPC for Cd, selected genes based on literature research, independent of the
857 approach described above. As a second independent approach, we used the same group of
858 genes to calculate a "Gene score" for each strain by summing up all genes (each + 1) and their
859 additional gene copies (each + 1) present in the genome using the `mutate()` function from
860 the *tidyverse* package. The `cor.test()` function was used to test for a correlation between
861 "Gene score" and Cd tolerance (MPC) using Kendall's rank correlation, and the results were
862 plotted using the `ggplot()` function from the *ggplot2* package.

863 # Acknowledgements

864 We thank Prof. Dr. Franz Narberhaus for access to 96-pin microplate replicator. We thank
865 Andreas Aufermann, Rebekka Fresen and Martin Pullack for assistance with plant cultivation
866 and Petra Düchting for contributing her expertise and for conducting all multi-element
867 analyses.

868 # Figure legends

869 **Figure 1. Metal(loid) tolerances of phyllosphere bacterial strains in relation to the leaf**
870 **apoplastic fluid ionome of *A. thaliana*. (A, B)** Metal(loid) dose-response curves for the
871 phyllosphere bacterial collection (A, *At*-LSPHERE, n = 224 strains) and for a bacterial strain
872 collection from unplanted soils (B, n = 25) (Bai et al. 2015). Each strain was spotted on agar-
873 solidified R2A medium supplemented with a series of metal(loid) concentrations. Replicate
874 data points represent independent experiments; lines are curve fits (see Methods, Data S1). **(C)**
875 Cd tolerance of synthetic bacterial communities (SynComs; datapoints shown by circles, bars
876 mark mean ± SD, n = 6 technical replicates; data from one experiment representative of a total
877 of four independent experiments). Apparent doubling times of the SynComs were calculated
878 based on the earliest identifiable log phase of growth from time series of OD_{600} measurements
879 with cultivation at 26°C for 24 h (see Figure S3). ∞: no growth. Note that the horizontal axis
880 is not scaled. **(D)** Ionome of leaf apoplastic fluid (AF_{EDTA}, blue line), and of the entire fresh

881 leaf ($Leaf_{Total}$, red line). Shown is the average (line) and the standard deviation (shadow) for
882 each element as Log_{10} of the concentration ([mM] for Ca, S, P, Mg, and K; [µM] for Zn, Mo,
883 Mn, Fe, Cu, and Cd; $n = 4$ samples for AF and $n = 3$ samples for leaves). **(E)** Boxplots showing
884 metal concentrations in apoplastic fluid (AF_{EDTA}, AF_{Water}: extracted in 100 µM EDTA and in
885 water, respectively) of soil-grown plants, alongside metal tolerance of the *At*-LSPHERE
886 collection (re-plotted from (A)). For AF, boxes show median (central line), 25%/75%ile (box),
887 and maximum/minimum (bars) of all measurements ($n = 17$; see Table S5, Figure S4E-G). For
888 metal tolerances, boxes show effective concentration EC_{50} (central line), EC_{25}/EC_{75} (boxes)
889 and EC_{1-5}/EC_{95-99} (bars)(see Table 1, and Materials and Methods). Dose-response curves are
890 from a minimum of 3 independent experiments conducted on R2A medium (A, B). AF data
891 are from one representative experiment (D; Table S5, GHs 4; Figure S4E-G, E4) and from 4
892 independent experiments conducted on greenhouse soil (E). Not shown: AF_{Water} for Cd and
893 data for As were below our detection limits (D, E).

894 **Figure 2. Metal(loid) tolerance profiles of keystone strains of the *A. thaliana* phyllosphere**
895 **bacterial community**. **(A)** Profiles of maximum permissive concentrations (MPC) normalized
896 to EC_{50} on solid R2A media. Shown are median values (connected by black lines), with minima
897 and maxima (grey shadows, $n = 3$ independent experiments), on a Log_{10} scale (1 reflects an
898 MPC equivalent to EC_{50}, see Table 1, Data S1). Values below 0.5 (small red)/0.05 (large red)
899 and above 5 (small blue) are shown as colored circular shapes. Mn is not shown because of its
900 low toxicity in these strains. **(B, C)** Combined toxicity effects of Cd and Cu (B), and Cd, Zn,
901 and Mn (C) on keystone strains in liquid R2A media (see Tables S8 and S9). Symbols show
902 combined toxicity-enhancing (+) and toxicity-alleviating (-) effects of the metals connected by
903 the corresponding black line; numbers are concentrations [µM]. Results reproduced in
904 three/two out of three independent experiments are shown in black/grey color. Grey dotted
905 lines: effect of the adjacent metal on the combined toxicity of the other two metals (C). Data
906 not shown (n.e.: results could not be evaluated because of metal sensitivity, B). Circle sizes
907 adjusted to fit.

908 **Figure 3. Effects of metal(loid) tolerances of *At*-LSPHERE bacterial strains on the**
909 **phylogenetic structure among the survivors.** Pie fractions reflect the percentage share (with
910 the number given in white) out of all bacterial strains that were able to grow under a given
911 condition (Data S1). The metal(loid) concentration is given in black fonts above the chart for

912 each treatment. *Significant enrichment (black) or depletion (white) compared to the control
913 condition (*q-value* < 0.05).

914 **Figure 4. Hierarchical clustering of strains according to their metal(loid) tolerance**
915 **profiles.** Maximum permissive concentrations of Cd, Zn, Cu, arsenite, and Mn in the *At*-
916 LSPHERE strains (Data S1) were clustered by Euclidean distance-based (Ward) clustering (*z*-
917 score-based). Clusters (I to X) are emphasized by different colors (left) and separated by
918 horizontal lines. Symbols mark the positions of *Rhodococcus (n* = 6), *Pseudomonas* (*n* = 9),
919 *Rhizobium* (*n* = 15), and keystone strains (*n* = 4).

920 **Figure 5. Strain-specific metal(loid) tolerances shown over the phylogeny of the *At*-**
921 **LSPHERE strain collection.** Cladogram of the *At*-LSPHERE strain collection (*n* = 214; 16s
922 rRNA-based (Bai et al. 2015)) with circular heatmap representations of relative tolerance.
923 Heatmap color shade reflects strain-wise maximum permissive concentrations (MPC, median
924 of *n* = 3 independent experiments; Data S1) normalized to the EC_{50}, the concentration
925 eliminating the growth of 50% of all bacterial strains (Cd: 0.049 mM, Zn: 0.5 mM, Cu: 0.4
926 mM, As^{III}: 1.1 mM, Mn: 9.2 mM; Table 1). Strains (*n* = 8) not profiled for metal tolerance are
927 marked by a black line around the colored circle.

928 **Figure 6. Relationships between known Cd tolerance genes and Cd tolerance of *At*-**
929 **LSPHERE strains. (A)** PCA of strain-wise maximum permissive Cd concentrations (MPC, *z*-
930 score-based) and presence/absence of known Cd tolerance-related genes. Each datapoint
931 represents one strain (Data S1-S3). The percentages of variation accounted for by each
932 significant PC are given in parentheses (95% confidence intervals: PC 1, 31% to 36.7%; PC 2,
933 10.9% to 13.8%; bootstrapping with 999 replicates). KEGG Orthology (KO) identifiers with
934 significant loadings on PC1 are: *czcA–D* and *tolC* (alternative short names linked by "..."; Data
935 S6). **(B)** Plot of strain-wise maximum permissive Cd concentration (MPC, absolute) against a
936 gene score incorporating both presence/absence and copy number of known Cd tolerance-
937 related genes. Each datapoint represents one strain (Data S1-S3). The gene score of a strain is
938 the genome-wide sum of genes with previously published roles in Cd tolerance (see A), with
939 additional gene copies also counted (Kendall's rank correlation, $\tau = 0.31$, $p = 3.5\times10^{-9}$; Data
940 S7).

941 **Figure 7. Metal(loid)-related genes implicated in Cd tolerance of *At*-LSPHERE strains**
942 **shown over phylogeny.** Shown are known metal(loid)-related genes of which the presence in

943 the genome was statistically associated with altered Cd tolerance in our study ($p_{adj} < 0.005$, for
944 *arsH* $p_{adj} = 0.023$; with Bonferroni corrections). Colors of KO identifiers reflect whether the
945 median of maximum permissive concentrations (MPC median) of all positive strains was > 2-
946 fold higher (red) or > 2-fold lower (blue) than that of all strains lacking an orthologue (Data
947 S4; else KO id. not shown). Genes (KO identifiers) are only shown if present in at least 30
948 bacterial strains (Data S4). Strains ($n = 8$) not profiled for metal tolerance are marked by a
949 black line around the colored circle.

950 # References

951 Abou-Shanab, R. A., P. van Berkum, and J. S. Angle. 2007. 'Heavy metal resistance and
952 genotypic analysis of metal resistance genes in gram-positive and gram-negative
953 bacteria present in Ni-rich serpentine soil and in the rhizosphere of *Alyssum murale*',
954 *Chemosphere*, 68: 360-7.
955 Achard-Joris, M., H. B. van den Berg van Saparoea, A. J. Driessen, and J. P. Bourdineaud.
956 2005. 'Heterologously expressed bacterial and human multidrug resistance proteins
957 confer cadmium resistance to *Escherichia coli*', *Biochemistry*, 44: 5916-22.
958 Achard, Maud E. S., Sian L. Stafford, Nilesh J. Bokil, Jy Chartres, Paul V. Bernhardt, Mark
959 A. Schembri, Matthew J. Sweet, and Alastair G. McEwan. 2012. 'Copper
960 redistribution in murine macrophages in response to Salmonella infection', *Biochem J*,
961 444: 51-57.
962 Amoroso, M. J., G. R. Castro, F. J. Carlino, N. C. Romero, R. T. Hill, and G. Oliver. 1998.
963 'Screening of heavy metal-tolerant actinomycetes isolated from the Sali River', *J Gen*
964 *Appl Microbiol*, 44: 129-32.
965 Andersen, T. G., M. Barberon, and N. Geldner. 2015. 'Suberization - the second life of an
966 endodermal cell', *Curr Opin Plant Biol*, 28: 9-15.
967 Bai, Y., D. B. Müller, G. Srinivas, R. Garrido-Oter, E. Potthoff, M. Rott, N. Dombrowski, P.
968 C. Münch, S. Spaepen, M. Remus-Emsermann, B. Hüttel, A. C. McHardy, J. A.
969 Vorholt, and P. Schulze-Lefert. 2015. 'Functional overlap of the Arabidopsis leaf and
970 root microbiota', *Nature*, 528: 364-9.
971 Barberon, M., J. E. Vermeer, D. De Bellis, P. Wang, S. Naseer, T. G. Andersen, B. M.
972 Humbel, C. Nawrath, J. Takano, D. E. Salt, and N. Geldner. 2016. 'Adaptation of Root
973 Function by Nutrient-Induced Plasticity of Endodermal Differentiation', *Cell*, 164:
974 447-59.
975 Beard, S. J., R. Hashim, J. MembrilloHernandez, M. N. Hughes, and R. K. Poole. 1997.
976 'Zinc(II) tolerance in *Escherichia coli* K-12: evidence that the *zntA* gene (o732)
977 encodes a cation transport ATPase', *Mol Microbiol*, 25: 883-91.
978 Bernal, María, David Casero, Vasantika Singh, Grandon T. Wilson, Arne Grande, Huijun
979 Yang, Sheel C. Dodani, Matteo Pellegrini, Peter Huijser, and Erin L. Connolly. 2012.
980 'Transcriptome sequencing identifies SPL7-regulated copper acquisition genes
981 FRO4/FRO5 and the copper dependence of iron homeostasis in Arabidopsis', *The*
982 *Plant Cell*, 24: 738-61.
983 Bulgarelli, D., K. Schlaeppi, S. Spaepen, E. Ver Loren van Themaat, and P. Schulze-Lefert.
984 2013. 'Structure and functions of the bacterial microbiota of plants', *Annu Rev Plant*
985 *Biol*, 64: 807-38.

Carlström, C. I., C. M. Field, M. Bortfeld-Miller, B. Müller, S. Sunagawa, and J. A. Vorholt. 2019. 'Synthetic microbiota reveal priority effects and keystone strains in the Arabidopsis phyllosphere', *Nat Ecol Evol*, 3: 1445-54.

Chandrangsu, Pete, Christopher Rensing, and John D. Helmann. 2017. 'Metal homeostasis and resistance in bacteria', *Nat Rev Microbiol*, 15: 338-50.

Chaoprasid, Paweena, Sumontha Nookabkaew, Rojana Sukchawalit, and Skorn Mongkolsuk. 2015. 'Roles of *Agrobacterium tumefaciens* C58 ZntA and ZntB and the transcriptional regulator ZntR in controlling Cd^{2+}/Zn^{2+}/Co^{2+} resistance and the peroxide stress response', *Microbiology*, 161: 1730-40.

Chen, T., K. Nomura, X. Wang, R. Sohrabi, J. Xu, L. Yao, B. C. Paasch, L. Ma, J. Kremer, Y. Cheng, L. Zhang, N. Wang, E. Wang, X. F. Xin, and S. Y. He. 2020. 'A plant genetic network for preventing dysbiosis in the phyllosphere', *Nature*, 580: 653-57.

Choudhury, R., and S. Srivastava. 2001. 'Zinc resistance mechanisms in bacteria', *Curr Sci*, 81: 768-75.

Clemens, Stephan. 2001. 'Molecular mechanisms of plant metal tolerance and homeostasis', *Planta*, 212: 475-86.

Cohen, C. K., D. F. Garvin, and L. V. Kochian. 2004. 'Kinetic properties of a micronutrient transporter from *Pisum sativum* indicate a primary function in Fe uptake from the soil', *Planta*, 218: 784-92.

Colina Blanco, A. E., E. Pischke, A. Higa Mori, C. F. Kerl, S. Clemens, and B. Planer-Friedrich. 2023. 'In Planta Arsenic Thiolation in Rice and *Arabidopsis thaliana*', *Environ Sci Technol*, 57: 21846-54.

Connolly, E. L., J. P. Fett, and M. L. Guerinot. 2002. 'Expression of the IRT1 metal transporter is controlled by metals at the levels of transcript and protein accumulation', *Plant Cell*, 14: 1347-57.

Dhankher, Om Parkash, Nupur A. Shasti, Barry P. Rosen, Mark Fuhrmann, and Richard B. Meagher. 2003. 'Increased cadmium tolerance and accumulation by plants expressing bacterial arsenate reductase', *New Phytol*, 159: 431-41.

Endo, G., and S. Silver. 1995. 'CadC, the transcriptional regulatory protein of the cadmium resistance system of *Staphylococcus aureus* plasmid pI258', *J Bacteriol*, 177: 4437-41.

Escudero, Viviana, Álvaro Castro-León, Darío Ferreira Sánchez, Isidro Abreu, María Bernal, Ute Krämer, Daniel Grolimund, Manuel González-Guerrero, and Lucía Jordá. 2022. '*Arabidopsis thaliana* Zn^{2+}-efflux ATPases HMA2 and HMA4 are required for resistance to the necrotrophic fungus *Plectosphaerella cucumerina* BMM', *J Exp Bot*, 73(1):339-350.

Farvardin, A., A. I. Gonzalez-Hernandez, E. Llorens, P. Garcia-Agustin, L. Scalschi, and B. Vicedo. 2020. 'The Apoplast: A Key Player in Plant Survival', *Antioxidants*, 9.

Figueiredo, J., A. R. Cavaco, L. Guerra-Guimaraes, C. Leclercq, J. Renaut, J. Cunha, J. Eiras-Dias, C. Cordeiro, A. R. Matos, M. Sousa Silva, and A. Figueiredo. 2021. 'An apoplastic fluid extraction method for the characterization of grapevine leaves proteome and metabolome from a single sample', *Physiol Plant*, 171: 343-57.

Frawley, E. R., M. L. V. Crouch, L. K. Bingham-Ramos, H. F. Robbins, W. L. Wang, G. D. Wright, and F. C. Fang. 2013. 'Iron and citrate export by a major facilitator superfamily pump regulates metabolism and stress resistance in *Salmonella typhimurium*', *Proc Natl Acad Sci USA*, 110: 12054-59.

Geilfus, Christoph-Martin. 2017. 'The pH of the apoplast: dynamic factor with functional impact under stress', *Mol Plant*, 10: 1371-86.

1034 Geilfus, Christoph-Martin, Li Wang, Jiawen Wu, and Cheng Xue. 2020. 'The pH of the leaf
1035 apoplast is critical for the formation of *Pseudomonas syringae*-induced lesions on
1036 leaves of the common bean (*Phaseolus vulgaris*)', *Plant Sci*, 290: 110328.
1037 Hemmerle, L., B. A. Maier, M. Bortfeld-Miller, B. Ryback, C. G. Gabelein, M. Ackermann,
1038 and J. A. Vorholt. 2022. 'Dynamic character displacement among a pair of bacterial
1039 phyllosphere commensals *in situ*', *Nat Commun*, 13: 2836.
1040 Hörger, A. C., H. N. Fones, and G. M. Preston. 2013. 'The current status of the elemental
1041 defense hypothesis in relation to pathogens', *Front Plant Sci*, 4: 395.
1042 Kajala, K., K. L. Walker, G. S. Mitchell, U. Krämer, S. R. Cherry, and S. M. Brady. 2019.
1043 'Real-time whole-plant dynamics of heavy metal transport in *Arabidopsis halleri* and
1044 *Arabidopsis thaliana* by gamma-ray imaging', *Plant Direct*, 3: e00131.
1045 Kaur, U. J., A. Chopra, S. Preet, K. Raj, K. K. Kondepudi, V. Gupta, and P. Rishi. 2021.
1046 'Potential of 1-(1-napthylmethyl)-piperazine, an efflux pump inhibitor against
1047 cadmium-induced multidrug resistance in *Salmonella enterica* serovar *typhi* as an
1048 adjunct to antibiotics', *Braz J Microbiol*, 52: 1303-13.
1049 Kazemi-Dinan, A., S. Thomaschky, R. J. Stein, U. Krämer, and C. Müller. 2014. 'Zinc and
1050 cadmium hyperaccumulation act as deterrents towards specialist herbivores and
1051 impede the performance of a generalist herbivore', *New Phytol*, 202: 628-39.
1052 Kim, H. S., D. Nagore, and H. Nikaido. 2010. 'Multidrug efflux pump MdtBC of *Escherichia*
1053 *coli* is active only as a B2C heterotrimer', *J Bacteriol*, 192: 1377-86.
1054 Krämer, U. 2024. 'Metal Homeostasis in Land Plants: A Perpetual Balancing Act Beyond the
1055 Fulfilment of Metalloproteome Cofactor Demands', *Annu Rev Plant Biol*, 75: 27-65.
1056 Küpper, H., E. Lombi, F. J. Zhao, and S. P. McGrath. 2000. 'Cellular compartmentation of
1057 cadmium and zinc in relation to other elements in the hyperaccumulator *Arabidopsis*
1058 *halleri*', *Planta*, 212: 75-84.
1059 Legatzki, Antje, Sylvia Franke, Susann Lucke, Toni Hoffmann, Andreas Anton, Dieter
1060 Neumann, and Dietrich H. Nies. 2003. 'First step towards a quantitative model
1061 describing Czc-mediated heavy metal resistance in *Ralstonia metallidurans*',
1062 *Biodegradation*, 14: 153-68.
1063 Li, Lingjuan, Qiang Lin, Tiezhu Li, Xiaohong He, Shuming Peng, and Yong Tao. 2020.
1064 'Transcriptional response of *Pseudomonas chenduensis* strain MBR to cadmium
1065 toxicity', *Appl Microbiol Biotechnol*, 104: 9749-57.
1066 Lopez-Maury, L., F. J. Florencio, and J. C. Reyes. 2003. 'Arsenic sensing and resistance
1067 system in the cyanobacterium *Synechocystis* sp. strain PCC 6803', *J Bacteriol*, 185:
1068 5363-71.
1069 Marschner, Horst, and Petra Marschner. 2012. *Marschner's mineral nutrition of higher plants*
1070 (Elsevier/Academic Press: London ; Waltham, MA).
1071 Müller, D. B., O. T. Schubert, H. Rost, R. Aebersold, and J. A. Vorholt. 2016. 'Systems-level
1072 Proteomics of Two Ubiquitous Leaf Commensals Reveals Complementary Adaptive
1073 Traits for Phyllosphere Colonization', *Mol Cell Proteomics*, 15: 3256-69.
1074 Müller, D. B., C. Vogel, Y. Bai, and J. A. Vorholt. 2016. 'The Plant Microbiota: Systems-
1075 Level Insights and Perspectives', *Annu Rev Genet*, 50: 211-34.
1076 Murdoch, C. C., and E. P. Skaar. 2022. 'Nutritional immunity: the battle for nutrient metals at
1077 the host-pathogen interface', *Nat Rev Microbiol*, 20: 657-70.
1078 Nagakubo, S., K. Nishino, T. Hirata, and A. Yamaguchi. 2002. 'The putative response
1079 regulator BaeR stimulates multidrug resistance of *Escherichia coli* via a novel
1080 multidrug exporter system, MdtABC', *J Bacteriol*, 184: 4161-7.
1081 Nathan, Carl, and Michael U. Shiloh. 2000. 'Reactive oxygen and nitrogen intermediates in
1082 the relationship between mammalian hosts and microbial pathogens', *Proc Natl Acad*
1083 *Sci U S A*, 97: 8841-48.

Nieboer, E., and Richardson, D.H.S. 1980. 'The replacement of the nondescript term “heavy metals” by a biologically and chemically significant classification of metal ions', *Environ Poll Series B - Chem Phys 1, 3-26*.

Nies, D. H. 1992a. 'CzcR and CzcD, gene products affecting regulation of resistance to cobalt, zinc, and cadmium (czc system) in *Alcaligenes eutrophus*', *J Bacteriol*, 174: 8102-10.

———. 1992b. 'Resistance to cadmium, cobalt, zinc, and nickel in microbes', *Plasmid*, 27: 17-28.

Nies, D. H., A. Nies, L. Chu, and S. Silver. 1989. 'Expression and nucleotide sequence of a plasmid-determined divalent cation efflux system from *Alcaligenes eutrophus*', *Proc Natl Acad Sci USA*, 86: 7351-5.

Nies, D. H., and S. Silver. 1989. 'Plasmid-determined inducible efflux is responsible for resistance to cadmium, zinc, and cobalt in *Alcaligenes eutrophus*', *J Bacteriol*, 171: 896-900.

Nies, Dietrich H., and Gregor Grass. 2009. 'Transition metal homeostasis', *EcoSal Plus*, 3: 10-1128.

Nieto, J. J., A. Ventosa, and F. Ruiz-Berraquero. 1987. 'Susceptibility of halobacteria to heavy metals', *Appl Environ Microbiol*, 53: 1199-202.

Nishino, K., E. Nikaido, and A. Yamaguchi. 2007. 'Regulation of multidrug efflux systems involved in multidrug and metal resistance of *Salmonella enterica* serovar *typhimurium*', *J Bacteriol*, 189: 9066-75.

Norvell, W. A. 1991. 'Reactions of Metal Chelates in Soils and Nutrient Solutions.' in, *Micronutrients in Agriculture*.

O'Leary, B. M., A. Rico, S. McCraw, H. N. Fones, and G. M. Preston. 2014. 'The infiltration-centrifugation technique for extraction of apoplastic fluid from plant leaves using *Phaseolus vulgaris* as an example', *J Vis Exp*: 52113.

Outten, C. E., F. W. Outten, and T. V. O'Halloran. 1999. 'DNA distortion mechanism for transcriptional activation by ZntR, a Zn(II)-responsive MerR homologue in *Escherichia coli*', *J Biol Chem*, 274: 37517-24.

Pais, István, and J. Benton Jones. 1997. *The handbook of trace elements* (St. Lucie Press: Boca Raton, Fla.).

Pfeilmeier, S., G. C. Petti, M. Bortfeld-Miller, B. Daniel, C. M. Field, S. Sunagawa, and J. A. Vorholt. 2021. 'The plant NADPH oxidase RBOHD is required for microbiota homeostasis in leaves', *Nat Microbiol*, 6: 852-64.

Rensing, C., B. Mitra, and B. P. Rosen. 1997. 'The *zntA* gene of *Escherichia coli* encodes a Zn(II)-translocating P-type ATPase', *Proc Natl Acad Sci USA*, 94: 14326-31.

Ritpitakphong, U., L. Falquet, A. Vimoltust, A. Berger, J. P. Metraux, and F. L'Haridon. 2016. 'The microbiome of the leaf surface of Arabidopsis protects against a fungal pathogen', *New Phytol*, 210: 1033-43.

Robb, J., S. W. Lee, R. Mohan, and P. E. Kolattukudy. 1991. 'Chemical characterization of stress-induced vascular coating in tomato', *Plant Physiol*, 97: 528-36.

Robbins, Chanz, Thorsten Thiergart, Stéphane Hacquard, Ruben Garrido-Oter, Wolfgang Gans, Edgar Peiter, Paul Schulze-Lefert, and Stijn Spaepen. 2018. 'Root-associated bacterial and fungal community profiles of *Arabidopsis thaliana* are robust across contrasting soil P levels', *Phytobiomes*, 2: 24-34.

Samanovic, Marie I., Chen Ding, Dennis J. Thiele, and K. Heran Darwin. 2012. 'Copper in microbial pathogenesis: meddling with the metal', *Cell Host Microbe*, 11: 106-15.

Sattelmacher, B. 2001. 'The apoplast and its significance for plant mineral nutrition', *New Phytol*, 149: 167-92.

Silver, S., and M. Walderhaug. 1992. 'Gene regulation of plasmid- and chromosome-determined inorganic ion transport in bacteria', *Microbiol Rev*, 56: 195-228.

Singh, V. K., A. Xiong, T. R. Usgaard, S. Chakrabarti, R. Deora, T. K. Misra, and R. K. Jayaswal. 1999. 'ZntR is an autoregulatory protein and negatively regulates the chromosomal zinc resistance operon *znt* of *Staphylococcus aureus*', *Mol Microbiol*, 33: 200-7.

Stein, R. J., S. Höreth, J. R. de Melo, L. Syllwasschy, G. Lee, M. L. Garbin, S. Clemens, and U. Krämer. 2017. 'Relationships between soil and leaf mineral composition are element-specific, environment-dependent and geographically structured in the emerging model *Arabidopsis halleri*', *New Phytol*, 213: 1274-86.

Sterckeman, Thibault, and Sébastien Thomine. 2020. 'Mechanisms of Cadmium Accumulation in Plants', *Crit Rev Plant Sci*, 39: 322-59.

Tada, Y., and T. Inoue. 2000. 'Use of oligotrophic bacteria for the biological monitoring of heavy metals', *J Appl Microbiol*, 88: 154-60.

Torres, Miguel Angel, Jeffery L. Dangl, and Jonathan D. G. Jones. 2002. 'Arabidopsis gp91phox homologues AtrbohD and AtrbohF are required for accumulation of reactive oxygen intermediates in the plant defense response', *Proc Natl Acad Sci USA*, 99: 517-22.

Vert, G., N. Grotz, F. Dedaldechamp, F. Gaymard, M. L. Guerinot, J. F. Briat, and C. Curie. 2002. 'IRT1, an Arabidopsis transporter essential for iron uptake from the soil and for plant growth', *Plant Cell*, 14: 1223-33.

Vogel, C., N. Bodenhausen, W. Gruissem, and J. A. Vorholt. 2016. 'The Arabidopsis leaf transcriptome reveals distinct but also overlapping responses to colonization by phyllosphere commensals and pathogen infection with impact on plant health', *New Phytol*, 212: 192-207.

Vogel, C. M., D. B. Potthoff, M. Schafer, N. Barandun, and J. A. Vorholt. 2021. 'Protective role of the Arabidopsis leaf microbiota against a bacterial pathogen', *Nat Microbiol*, 6: 1537-48.

Vorholt, J. A. 2012. 'Microbial life in the phyllosphere', *Nat Rev Microbiol*, 10: 828-40.

White, Carine, Jaekwon Lee, Taiho Kambe, Kevin Fritsche, and Michael J. Petris. 2009. 'A role for the ATP7A copper-transporting ATPase in macrophage bactericidal activity', *J Biol Chem*, 284: 33949-56.

Williams, B. 2007. 'The chemistry of evolution: the development of our ecosystem', *Choice: Curr Rev Acad Libr* 44: 1197-97.

Xia, H., Y. Yu, Z. Chen, H. Liu, T. Wang, W. Huang, and Z. Chu. 2026. 'COPT4 interacts with COPT1 or COPT3 to manipulate the signaling response for copper-triggered immunity in Arabidopsis', *New Phytol*, in press.

Yang, Hung-Chi, and Barry P. Rosen. 2016. 'New mechanisms of bacterial arsenic resistance', *Biomed J*, 39: 5-13.

Zhao, C., Y. Zhang, Z. Chan, S. Chen, and S. Yang. 2015. 'Insights into arsenic multi-operons expression and resistance mechanisms in *Rhodopseudomonas palustris* CGA009', *Front Microbiol*, 6: 986.

Plewka-Mandelkow et al., Figure 1

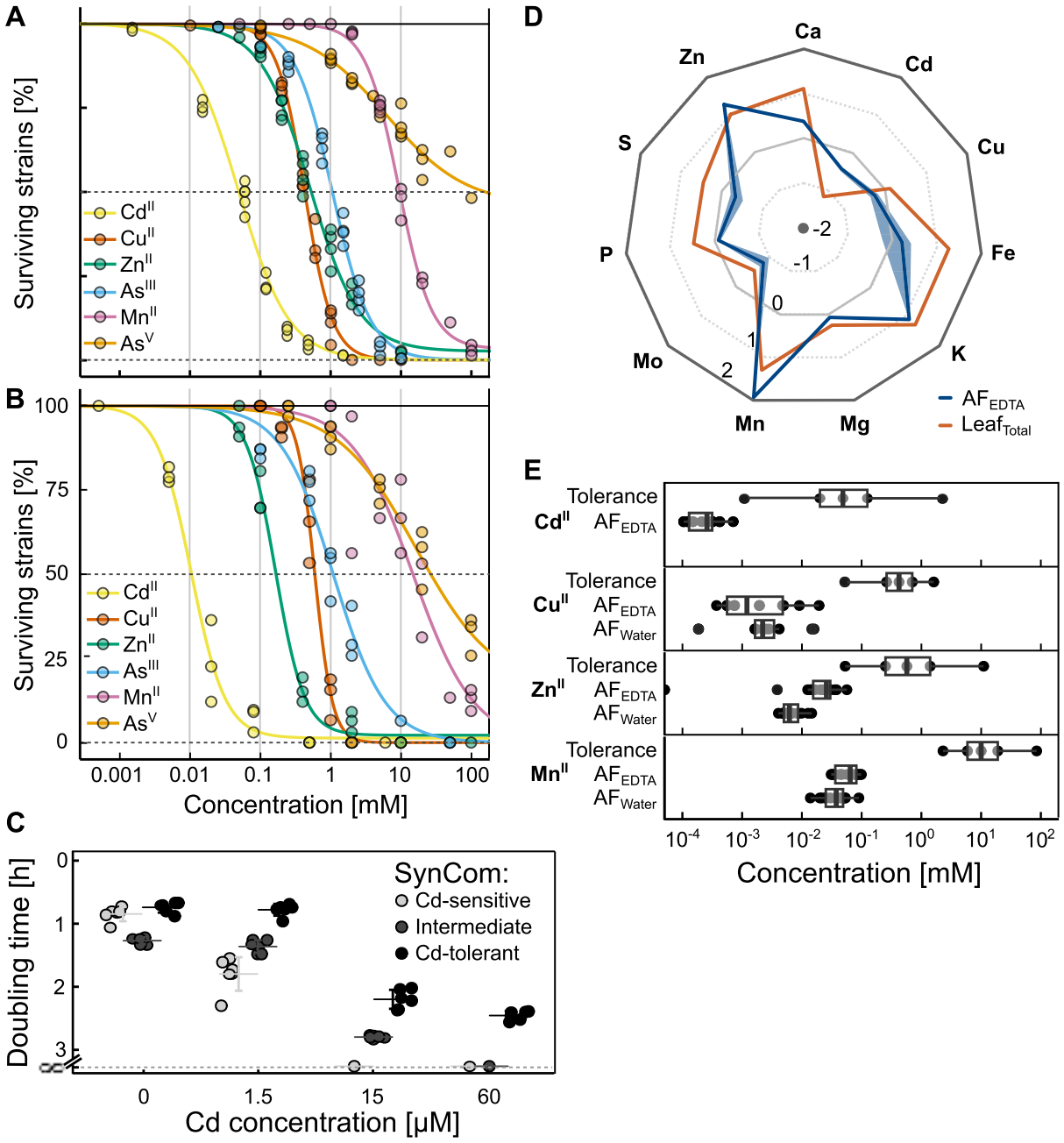

Plewka-Mandelkow et al., Figure 2

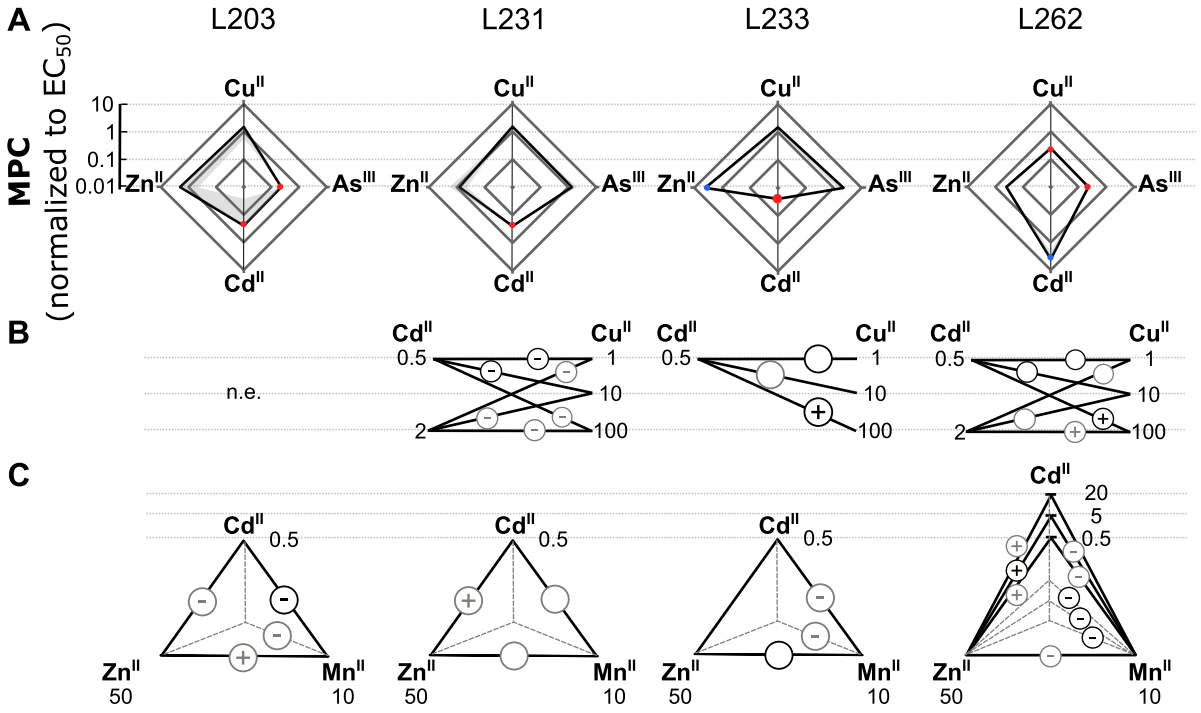

Plewka-Mandelkow et al., Figure 3

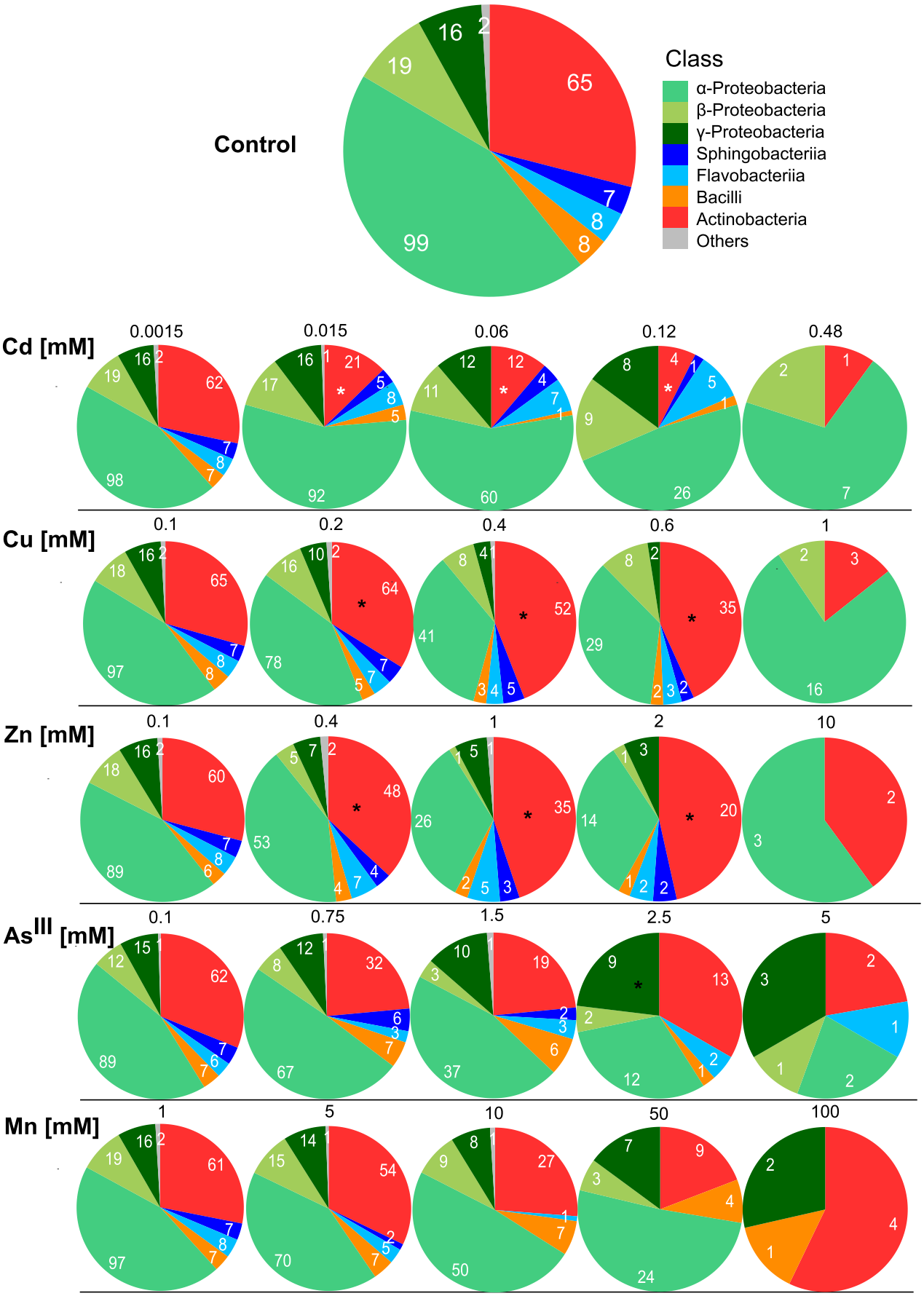

Plewka-Mandelkow et al., Figure 4

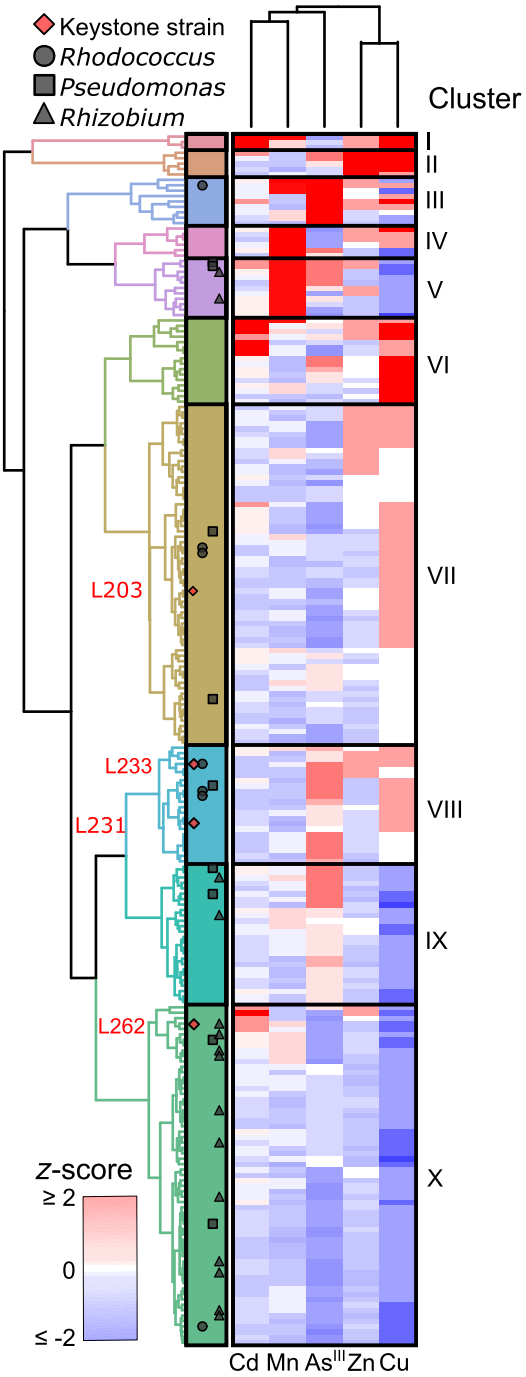

Plewka-Mandelkow et al., Figure 5

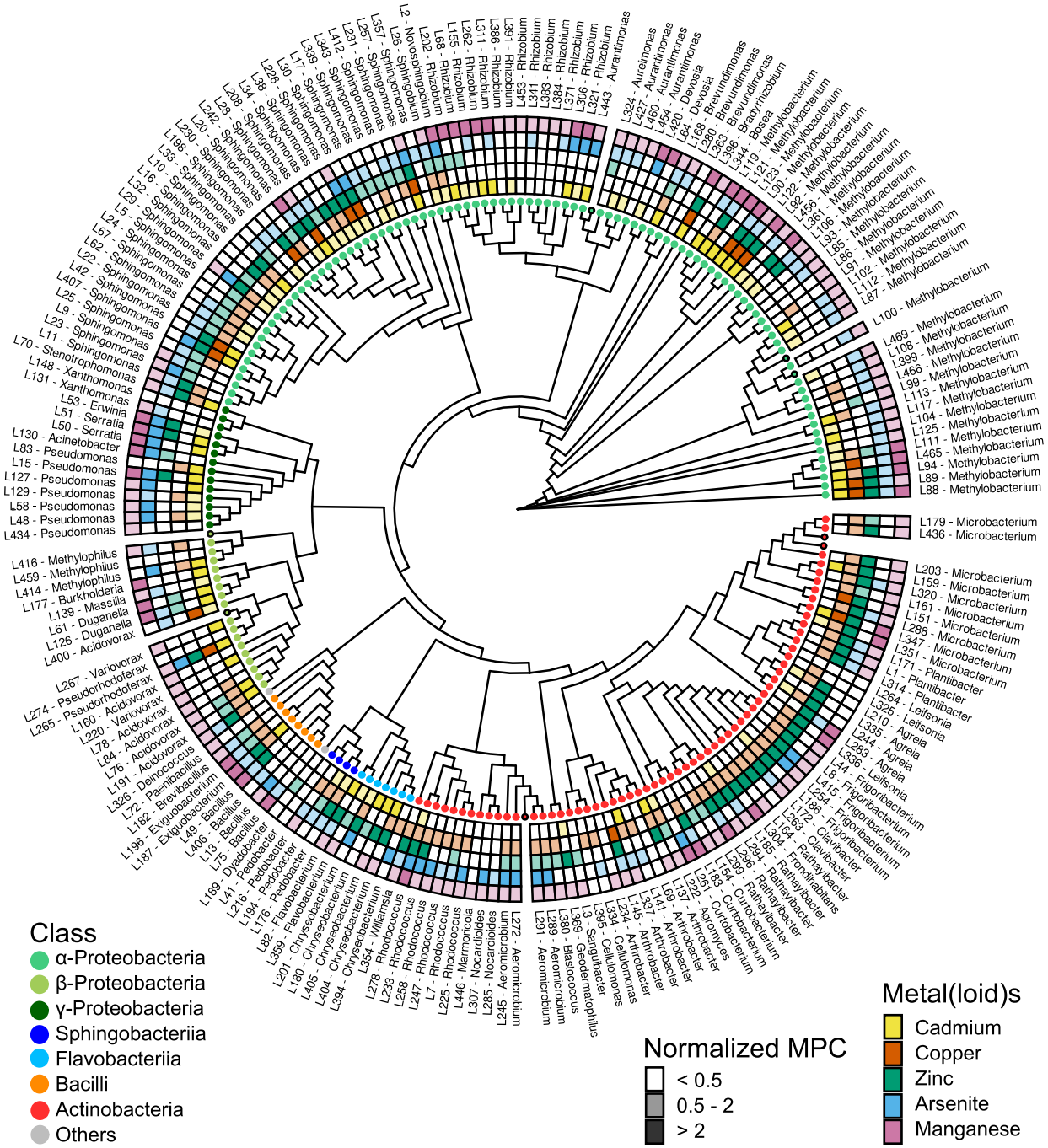

Plewka-Mandelkow et al., Figure 6

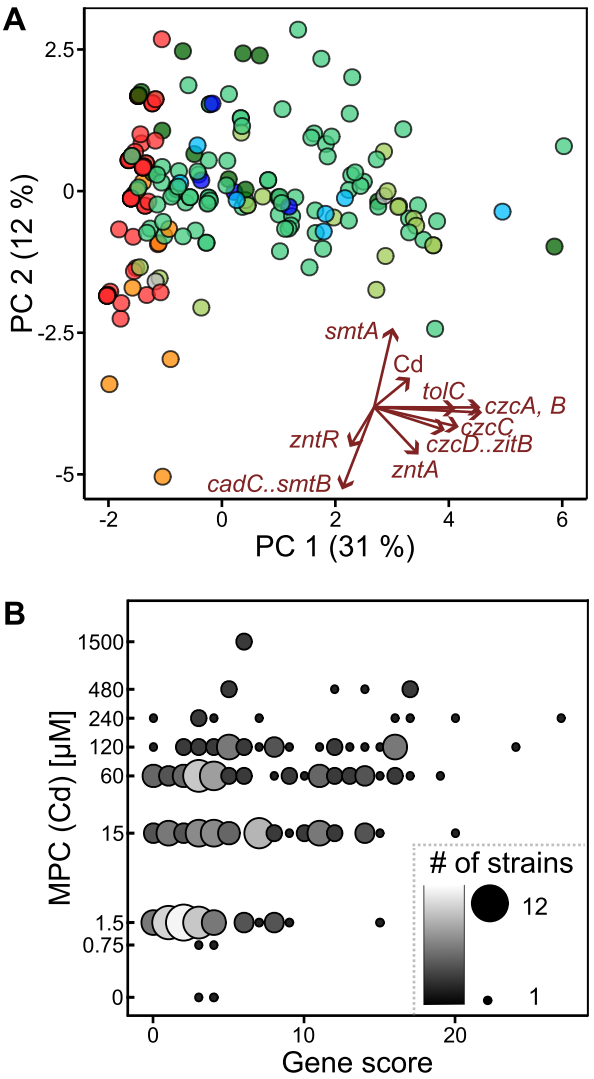
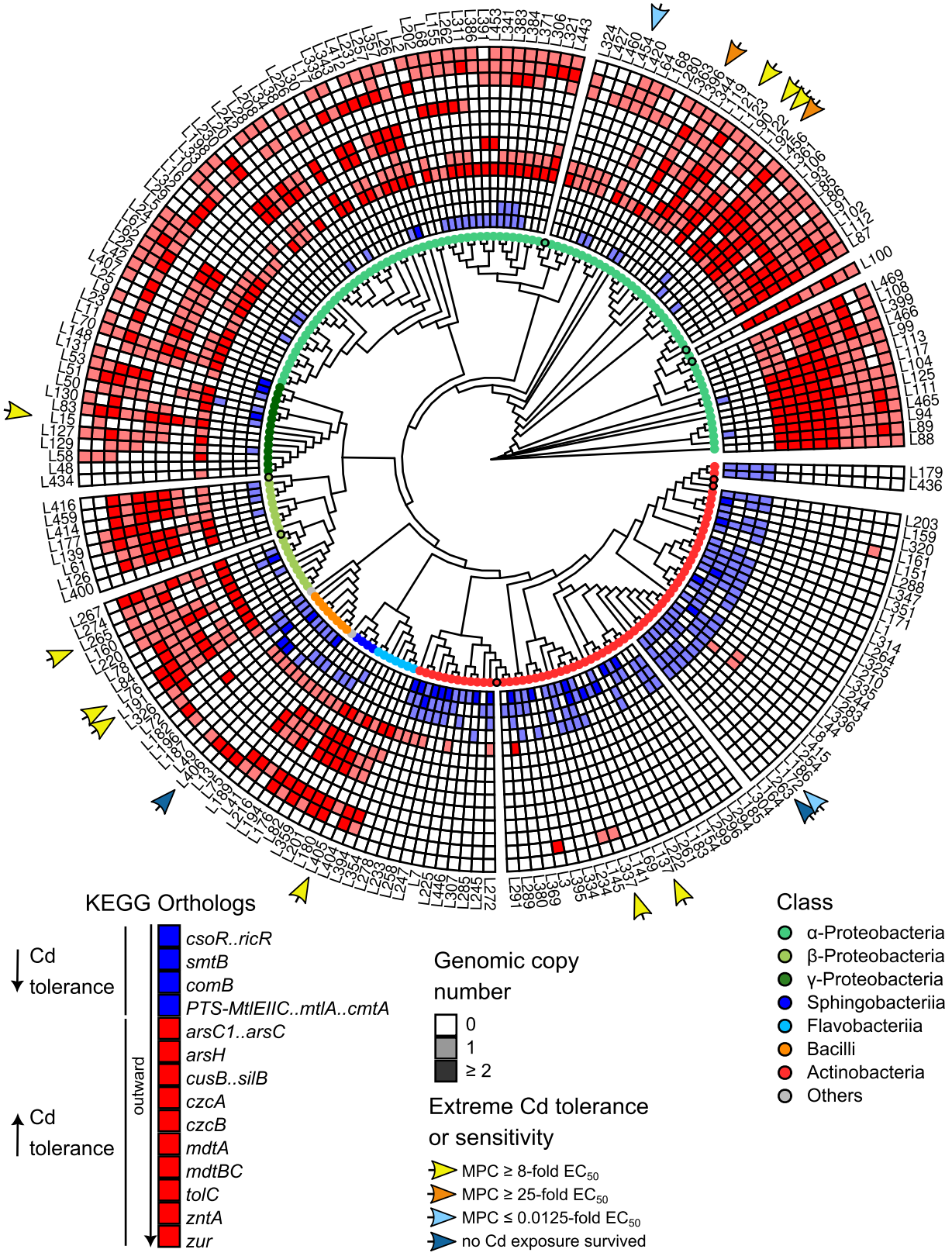
Plewka-Mandelkow et al., Figure 7